DTIC
SELECTED
JUN 0 8 1995
F

CRREL

Motion Resistance of Wheeled Vehicles in Snow

Paul W. Richmond

March 1995

19950607 016

DTIC QUALITY INSPECTED 5

Abstract

Before vehicle mobility in snow can be reliably predicted, a complete understanding of motion resistance in snow is required. This report examines several aspects of wheeled vehicle motion resistance using results obtained with the CRREL instrumented vehicle. Resistances of leading and trailing tires are examined. Limited data are presented for undercarriage drag, and third and fourth wheel passes in the same rut are initially analyzed, as is how snow deforms around a wheel. For the CRREL instrumented vehicle, a trailing tire has a resistance coefficient of about 0.017 for snow depths less than about 22 cm. For deeper snow, the disruption of the snowpack caused by a preceding wheel causes snow to fall into the rut, resulting in higher trailing tire coefficients. For larger vehicles, which in some cases have trailing tires carrying larger loads than preceding tires, the trailing tire coefficients are on the order of 0.048 and 0.025 for second and third trailing wheels respectively. Since there are no trailing tire data available for these larger vehicles, these values are based on nonlinear regression analysis, which includes a prediction of the leading tire resistance. The results and observations of this study are applied in a reanalysis of the towed resistance data obtained during the U.S. Army's Wheels vs. Tracks study. An improved algorithm is presented for predicting wheeled vehicle motion resistance caused by snow.

Cover: CRREL instrumented research vehicle in deep snow.

CRREL Report 95-7

**U.S. Army Corps
of Engineers**
Cold Regions Research &
Engineering Laboratory

Motion Resistance of
Wheeled Vehicles in Snow

Paul W. Richmond

March 1995

Accesion For		
NTIS CRA&I	☑	
DTIC TAB	☐	
Unannounced	☐	
Justification		
By		
Distribution /		
Availability Codes		
Dist	Avail and / or Special	
A-1		

DTIC QUALITY INSPECTED 5

PREFACE

The contents of this report are not to be used for advertising or promotional purposes. The citation of brand names does not constitute an official endorsement or approval of the use of such commercial products.

CONTENTS

ILLUSTRATIONS

TABLES

Table

NOMENCLATURE

Abbreviations

ANOVA	Analysis of variance
CIV	CRREL Instrumented research Vehicle
HMMWV	High-Mobility Multipurpose Wheeled Vehicle
HEMTT	Heavy Expanded Mobility Tactical Truck
LAV	Light Armored Vehicle

Symbols

a	arc length of the area of a wheel in contact with snow
h	snow depth
h_r	snow depth ratio, see eq 8
L_2	1/2 the load on the second axle
L_3	1/2 the load on the third axle
r	wheel radius
r^2	correlation coefficient
R_f	motion resistance at a front wheel
R_r	motion resistance at a rear wheel
R_s	motion resistance attributable to snow
V_f	vertical load on a front wheel
V_r	vertical load on a rear wheel
w	tire width
z	sinkage or rut depth of a wheel in snow
ρ_0	average undisturbed density
ρ_f	theoretical final density of the snow under a wheel

Motion Resistance of Wheeled Vehicles in Snow

PAUL W. RICHMOND

INTRODUCTION

Models of terrain–vehicle interaction require algorithms that can predict or estimate the resistance to motion caused by the terrain. As a vehicle moves through snow, it must overcome the resistance caused by snow deformation to maintain forward motion. There is resistance at each wheel or track. As a vehicle moves through undisturbed snow, the front wheels move and compact this snow. Succeeding or trailing wheels move over or through the snow compacted by the front wheels, presumably encountering a smaller resistance (since the snow has been compacted and moved out of the way). If the vehicle's undercarriage drags, this adds another source of resistance that must also be considered.

The motion resistance of a vehicle moving through snow is a very complex phenomenon, studied since the early 1940's. However, a robust, simple model of motion resistance due to snow has eluded researchers.

Currently, the U.S. Army uses in its mobility model an empirical equation for motion resistance in snow developed by Richmond et al. (1990). This equation is applicable to a large range of vehicles, both wheeled and tracked, and does not require elaborate measurements of snow properties. However, it is currently the weakest link of the overall Cold Regions Mobility Model (Richmond et al., in prep). When developing this equation, we analyzed a large quantity of total vehicle resistance data by dividing the whole vehicle resistance by the number of wheels, thus making the assumption that the trailing tire resistance was equal to the resistance of preceding wheels. This assumption was based on attempts to correlate data in which motion resistance was measured on one axle (CRREL Instrumented Vehicle [CIV]), on two axles (High Mobility Multipurpose Wheeled Vehicle [HMMWV]), and on four axles (Heavy Expanded Mobility Tactical Truck and Light Armored Vehicle [HEMTT and LAV]) during towing tests. This approach was not without basis, as the den- sity of the deformed snow behind each succeeding axle generally increased, although axle load did not. Density measurements in the wheel ruts (Table 1) were always well below what is considered the critical density of snow (0.5 to 0.55 Mg/m^3) (Yong and Fugue 1977), the point at which no further compaction by typically loaded vehicle traffic is observed. Additionally, Blaisdell (1987) made some limited indirect measurements of trailing tire re- sistance using the CIV and found that trailing tire resistance in snow could be as high as 84% of the leading tire resistance.

In an effort to increase the accuracy of the motion resistance model for undisturbed snow, a field study was conducted using the CIV with load cells installed on all four wheels. Prior to this work, only one set of load cells was available and these were installed on the front axle of the CIV (from 1981 to 1991). By use of the data acquired from these and other tests, a further understanding of the motion resistance of wheeled vehicles in snow was obtained, allowing an improved prediction algorithm to be presented.

EXPERIMENTAL PROCEDURE

The experimental procedure was designed around the capabilities of the CIV (Fig. 1 [Blaisdell 1983, Shoop 1992]). The instrumentation of the CIV was recently enhanced through the addition of load cells on the rear axle and a new data acquisition system based on a personal computer (Shoop et al. 1991). These triaxial load cells mea- sure longitudinal, vertical and lateral forces at the tire/terrain interface. Longitudinal forces repre- sent net traction or motion resistance, depending on whether the tire is driven or free rolling. Indi- vidual wheel and vehicle speeds are measured simultaneously with the wheel forces. By towing the CIV, resistance forces could be measured at all four wheels, and a tow hitch that could be placed off-center (Fig. 2) allowed the CIV to be towed through undisturbed snow.

Table 1. Vehicle sinkage and snow density data (after Richmond et al. 1990).

Vehicle	Contact pressure* (kPa)	Snow depth (cm)	Sinkage (cm)	Initial density (Mg/m³)	Rut density (Mg/m³)
HMMWV†	101.8	15.0	8.0	0.20	0.38
	123.3	15.0	8.0	0.20	0.48
	101.8	19.5	11.9	0.20	0.47
	123.3	19.5	13.8	0.20	0.50
	101.8	23.5	19.1	0.20	0.535
	123.3	23.5	21.0	0.20	—
	101.8	19.5	14.5	0.20	0.455
	123.3	17.5	13.1	0.20	0.470
	101.8	18.0	14.5	0.20	0.445
	123.3	18.0	13.0	0.20	0.475
	101.8	13.0	9.0	0.12	0.320
	123.3	12.0	8.5	0.12	0.410
	101.8	19.5	14.0	0.12	—
	123.3	18.0	14.0	0.12	—
	123.3	10.0	9.0	0.19	0.575
HEMTT**	233	20.0	12.4	0.25	0.490
	230	21.0	16.9	0.25	0.440
	225	20.0	16.2	0.25	0.520
	218	20.0	15.6	0.25	0.460
	233	16.5	12.4	0.25	0.490
	230	18.0	13.2	0.25	0.490
	225	20.5	15.4	0.25	0.510
	218	20.0	15.6	0.25	0.510
	233	20.0	14.3	0.245	—
	218	17.0	12.6	0.245	0.460
	233	13.0	10.0	0.12	—
HEMTT††	177	17.0	12.6	0.245	0.510
	174	18.0	15.1	0.245	0.525
	224	17.5	14.6	0.245	0.430
	212	16.0	13.1	0.245	0.455
	212	16.0	12.2	0.245	0.455
	212	4.0	3.0	0.095	—
	177	12.0	10.5	0.12	0.300
	212	11.0	9.0	0.12	0.315

*Contact pressure of the wheel behind which the rut density measurement was made.
†With an inflation pressure of 137.9 kPa (front) and 151.7 kPa (rear).
**With an inflation pressure of 241.3 kPa (front two axles), 275.8 kPa (rear two axles).
††With an inflation pressure of 137.9 kPa (front two axles) and 206.8 kPa (rear two axles).

Tests were conducted at the Keweenaw Research Center of the Michigan Technological University, in northern Michigan, during January and February 1993. The testing areas had been graded free of vegetation prior to any snowfall, and were nearly level. A layer of packed snow was beneath the undisturbed snow in which the tests were conducted. The CIV was equipped with Michelin LT 235XCH4 tires for these tests.

Initial tests were done with the tires inflated at 103 kPa (15 lb/in.²), while most of the tests were run at an inflation pressure of 179 kPa (26 lb/in.²). Tire data are in Table 2.

A static calibration procedure (Shoop 1992) was used. Prior to collecting data in the snow, we conducted at least four tests on hard surfaces. These hard surfaces were sometimes covered with packed snow or ice; however, an attempt was made to use areas that were as smooth as possible. These hard surface data were averaged for each load cell and used to remove from the subsequent snow resistance data the hard surface rolling resistance and any zero offset (remaining from the static calibration) in the load cells.

In these tests the vehicle was towed with all four hubs locked out. During initial calibration tests,

Figure 1. CRREL instrumented vehicle.

the effects of the disk brake pads on the hard surface rolling resistance values were examined. As long as the brakes were not applied during the hard surface tests, or during any subsequent tests, the calibration and hard surface values remained valid. It did not matter if the pads were installed or not, although the hard surface resistance is higher with the pads in place. By closing the valves in the CIV brake system, inadvertent braking can be avoided. Of course, with no effective brakes on the vehicle, care must be taken with the tow vehicle and tow hitch.

Most tests in undisturbed snow were conducted by towing the vehicle at about 5 km/hr using the off-set tow hitch shown in Figure 2. A few tests were done without towing the CIV, using the front wheels to drive the vehicle in deep snow. Additionally, some tests were conducted with the CIV

Figure 2. Off-center towing hitch.

3

Table 2. Tire deflection data.

Wheel location	Nominal load (N)	Deformed radius (cm)	Maximum undeformed radius (cm)	Maximum section width (cm)
Inflation pressure 103 kPa				
left front	6800	30.5	36.5	27.2
right front		30.0	36.5	27.2
left rear	5510	31.5	37.0	27.2
right rear		32.5	37.0	27.2
Inflation pressure 179 kPa				
left front	6800	33.0	36.7	25.6
right front		32.4	37.5	26.3
left rear	5510	33.5	37.5	25.5
right rear		34.2	38.0	25.5

following in the ruts made by the tow vehicle. After each test run, the undisturbed snow depths along both the left and right wheel ruts were measured at 1-m intervals. These data were later averaged to obtain an undisturbed snow depth value for each side of the vehicle. At the conclusion of a series of tests, several snow pits were used to characterize the snow and to determine an average density for each test.

RESULTS AND ANALYSIS

Table 3 contains a summary of the data collected. The data are separated into sets based on the day of the test and the tire inflation pressure. Initial snow depths ranged between 10 and 37 cm and average initial snow densities ranged from 0.11 to 0.25 Mg/m^3. All of the snow data collected are given in Appendix A.

Leading tire resistance

The leading tire data from Table 3 are plotted in Figure 3 using the resistance parameter ($\rho_0 aw$) in kilograms per meter, developed by Richmond et al. (1990). The variables in this parameter are illustrated in Figure 4; ρ_0 is the average initial undisturbed density of the snow, a is the arc length of the tire in contact with the snow, and w is the maximum tire width in meters. The arc length a is determined from the sinkage z and the tire radius, where the sinkage is determined from

$$z = h\left(1 - \frac{\rho_0}{\rho_f}\right) \tag{1}$$

where h is the snow depth, and ρ_f is the theoretical final density, which is determined from the following with p_{max} the maximum contact pressure:

$$\rho_f = 0.50 \text{ Mg/m}^3 \quad \text{for } p_{max} \leq 210 \text{ kPa}$$
$$\rho_f = 0.55 \text{ Mg/m}^3 \quad \text{for } p_{max} > 210 \text{ kPa}$$
$$\rho_f = 0.60 \text{ Mg/m}^3 \quad \text{for } p_{max} > 350 \text{ kPa}$$
$$\rho_f = 0.65 \text{ Mg/m}^3 \quad \text{for } p_{max} > 700 \text{ kPa}.$$

A value of 0.50 Mg/m^3 is used for the CIV with the inflation pressure and tires used in these tests.

Three equations are plotted on Figure 3. These are

$$R_s = 15.62 \, (\rho_0 aw)^{1.2676} \tag{2}$$

which is a fit of the data collected during the CIV tests reported herein

$$R_s = 11.25 \, (\rho_0 aw)^{1.58} \tag{3}$$

which was obtained for the CIV alone in 1988 and 1989 (Richmond et al. 1990) and

$$R_s = 68.083 \, (\rho_0 aw)^{0.9135} \tag{4}$$

which is the currently used shallow snow resistance equation (Richmond et al. 1990). R_s is the resistance per wheel (in Newtons) for a vehicle traveling through primarily undisturbed snow. Combining the old and new CIV data yields the following equation

$$R_s = 21.313 \, (\rho_0 aw)^{1.1918} \tag{5}$$

which has an r^2 value of 0.58 compared to 0.76 for

4

Table 3. CIV motion resistance data, 1993.

Set no.	Test no.	Velocity (km/hr)	Snow depth (cm)	Density (kg/m³)	Wheel sinkage (cm)	Radius (cm)	Width (cm)	Predicted sinkage* (cm)	Arc length (cm)	ap_ow (kg/m)	Resistance (N) Front	Rear	Vertical load (N) Front	Rear	Coefficient Front	Rear
1	0119g-r†	5.0	13.4	160	9.90	36.5	27.2	9.1	26.4	11.5	346.5	77.4	6931.2	5423.7	0.0500	0.0143
	0119g-l	5.0	15.5	160	12.0	36.5	27.2	10.5	28.5	12.4	416.4	46.7	6646.1	5453.5	0.0626	0.0086
	0119h-r	6.6	15	170	12.5	36.5	27.2	9.9	27.5	12.7	316.7	160.1	6886.7	5449.9	0.0460	0.0294
	0119h-l	6.6	18.6	170	15.1	36.5	27.2	12.3	30.8	14.3	557.4	165.5	6800.4	5400.6	0.0820	0.0306
2	0119o-r	5.1	16.3	160	13.3	37.5	26.3	11.1	29.6	12.5	498.6	90.7	7032.2	5262.2	0.0709	0.0172
	0119o-l	5.1	16.6	160	13.6	37.5	25.6	11.3	29.9	12.2	394.1	56.5	6787.5	5582.5	0.0581	0.0101
	0119p-r	8.7	18.3	170	15.3	37.5	26.3	12.1	31.0	13.8	460.8	97.9	7119.3	5133.7	0.0647	0.0191
	0119p-l	8.7	19.1	170	16.3	37.5	25.3	12.6	31.7	13.6	469.7	125.9	6775.9	5716.8	0.0693	0.0220
3	0122g-r	5.3	21.1	220	17.1	37.5	26.3	11.8	30.6	17.7	474.2	37.8	7071.3	5574.9	0.0671	0.0068
	0122g-l	5.3	20.8	220	16.8	37.5	25.6	11.6	30.4	17.1	621.0	42.7	6461.5	5443.7	0.0961	0.0078
	0122h-r	9.0	19.8	220	15.8	37.5	26.3	11.1	29.6	17.1	532.0	52.5	7146.0	5493.5	0.0744	0.0096
	0122h-l	9.0	20.5	220	16.8	37.5	25.6	11.5	30.1	17.0	747.3	48.9	6453.9	5454.8	0.1158	0.0090
	0122i-r	2.1	20.1	220	16.1	37.5	26.3	11.3	29.8	17.3	470.2	47.2	6716.8	5504.6	0.0700	0.0086
	0122i-l	2.1	20.5	220	16.5	37.5	25.6	11.5	30.1	17.0	635.6	10.2	6853.8	5554.0	0.0927	0.0018
	0122j-r	5.5	18	220	14.5	37.5	26.3	10.1	28.2	16.3	482.2	8.5	6876.0	5361.9	0.0701	0.0016
	0122j-l	5.5	19	220	15.5	37.5	25.6	10.6	29.0	16.3	693.5	0.0	6662.5	5695.9	0.1041	0.0000
4	0122o-r	5.0	21.2	220	16.2	36.5	27.2	11.9	30.3	18.1	414.1	109.9	7265.2	5845.8	0.0570	0.0188
	0122o-l	5.0	37.5	220	32.5	36.5	27.2	21.0	41.3	24.7	1176.5	139.2	6755.0	5007.3	0.1742	0.0278
	0122p-r	6.8	22.2	220	17.2	36.5	27.2	12.4	31.1	18.6	525.8	93.0	7296.4	5700.8	0.0721	0.0163
	0122p-l	6.8	20.5	220	15.5	36.5	27.2	11.5	29.8	17.8	451.5	64.9	6498.8	5236.4	0.0695	0.0124
	0122q-r	5.5	17.9	220	12.9	36.5	27.2	10.0	27.7	16.6	340.7	83.6	7071.3	5648.3	0.0482	0.0148
	0122q-l	5.5	17.8	220	12.8	36.5	27.2	10.0	27.6	16.5	374.5	57.4	6730.1	5315.2	0.0557	0.0108
	0122r-r	4.8	20.3	220	15.3	36.5	27.2	11.4	29.6	17.7	473.3	55.2	7058.0	5627.4	0.0671	0.0098
	0122r-l	4.8	20.7	220	15.7	36.5	27.2	11.6	29.9	17.9	480.9	92.1	6716.8	5371.6	0.0716	0.0171
	0122s-r	5.3	22.2	220	17.2	36.5	27.2	12.4	31.1	18.6	520.9	13.3	6794.6	5344.5	0.0767	0.0025
	0122s-l	5.3	21.6	220	16.6	36.5	27.2	12.1	30.6	18.3	456.8	37.8	7087.8	5574.0	0.0645	0.0068
	0122t-r	8.2	21.8	220	16.8	36.5	27.2	12.2	30.8	18.4	379.0	83.6	7101.1	5284.5	0.0534	0.0158
	0122t-l	8.2	22.9	220	17.9	36.5	27.2	12.8	31.6	18.9	505.8	82.3	6830.2	5578.0	0.0740	0.0148
5	0125f-r	6.0	35.7	160	30.7	37.5	25.6	24.3	45.4	18.6	1164.1	459.1	6994.8	5365.9	0.1664	0.0856
	0125g-l	4.7	36	160	31	37.5	25.6	24.5	45.6	18.7	1314.0	492.0	7202.5	5479.3	0.1824	0.0898
	0125h-l	7.6	32.4	160	27.4	37.5	25.6	22.0	43.0	17.6	-454.6**	368.3	6753.7	5747.1	-0.0673	0.0641
	0125h-r	7.6	31.6	160	26.6	37.5	26.3	21.5	42.4	17.8	-634.0	347.8	6804.4	6065.6	-0.0932	0.0573
	0125i-l	7.1	33.6	160	28.6	37.5	25.6	22.8	43.9	18.0	-492.7	368.3	6565.1	5796.9	-0.0751	0.0635
	0125i-r	7.1	33.6	160	28.6	37.5	26.3	22.8	43.9	18.5	-771.0	456.4	6963.7	5954.4	-0.1107	0.0766
6	0126e-l	4.7	12.2	110	0††	37.5	25.6	—	—	—	54.3	46.7	6897.8	5298.3	0.0079	0.0088
	0126e-r	4.7	11.2	110	0	37.5	26.3	—	—	—	93.0	3.1	6811.1	5417.0	0.0136	0.0006
	0126f-l	8.4	14.2	110	0	37.5	25.6	—	—	—	74.7	60.5	7004.6	5510.9	0.0107	0.0110
	0126f-r	8.4	12.8	110	0	37.5	26.3	—	—	—	104.1	36.9	6728.8	5270.2	0.0155	0.0070

5

Table 3 (cont'd). CIV motion resistance data, 1993.

Set no.	Test no.	Velocity (km/hr)	Snow depth (cm)	Density (kg/m³)	Wheel sinkage (cm)	Radius (cm)	Width (cm)	Predicted sinkage* (cm)	Arc length (cm)	apσw (kg/m)	Resistance (N)		Vertical load (N)		Coefficient	
											Front	Rear	Front	Rear	Front	Rear
7	0126g-l	5.0	13.6	110	9.6	37.5	25.6	10.6	28.9	8.1	167.7	85.0	6968.4	5217.7	0.0241	0.0163
	0126g-r	5.0	12.7	110	8.7	37.5	26.3	9.9	27.9	8.1	182.8	79.6	6907.1	5495.7	0.0265	0.0145
	0126h-l	9.5	16.7	110	13.7	37.5	25.6	13.0	32.2	9.1	229.5	151.2	6865.1	5139.5	0.0334	0.0294
	0126h-r	9.5	16.1	110	12.1	37.5	26.3	12.6	31.6	9.1	275.8	170.4	7068.3	5538.5	0.0390	0.0308
	0126i-l	5.1	17.6	110	15.1	37.5	25.6	13.7	33.2	9.3	213.1	74.7	6759.3	5281.4	0.0315	0.0141
	0126i-r	5.1	15.7	110	12.2	37.5	26.3	12.2	31.2	9.0	418.6	78.7	7199.0	5427.6	0.0581	0.0145
8	0202f-l	3.4	18.5	250	0	37.5	25.6	—	—	—	654.8	167.3	6536.6	5509.5	0.1002	0.0304
	0202f-r	3.4	13.2	250	0	37.5	26.3	—	—	—	311.8	0.0	7513.9	5294.2	0.0415	0.0000
9	0202g-l	4.2	16.1	230	13	37.5	25.6	8.7	26.1	15.3	876.7	115.7	6898.3	5362.3	0.1271	0.0216
	0202g-r	4.2	12.8	230	5	37.5	26.3	6.9	23.1	14.0	521.3	138.3	7196.3	5609.2	0.0724	0.0247
	0202h-l	5.8	18.6	230	8.5	37.5	25.6	10.0	28.1	16.5	831.8	327.4	7005.5	5130.1	0.1187	0.0638
	0202h-r	5.8	10.8	230	9	37.5	26.3	5.8	21.2	12.8	435.0	240.2	7200.3	5839.2	0.0604	0.0411

*Predicted sinkage based on eq 1.
†Month and day of test are first four digits; last character (l,r) indicates whether data are from left or right side of vehicle.
**Traction measurements are shown as negative values.
††Measured wheel sinkage was zero because the CIV wheels traveled in the ruts of the tow vehicle.
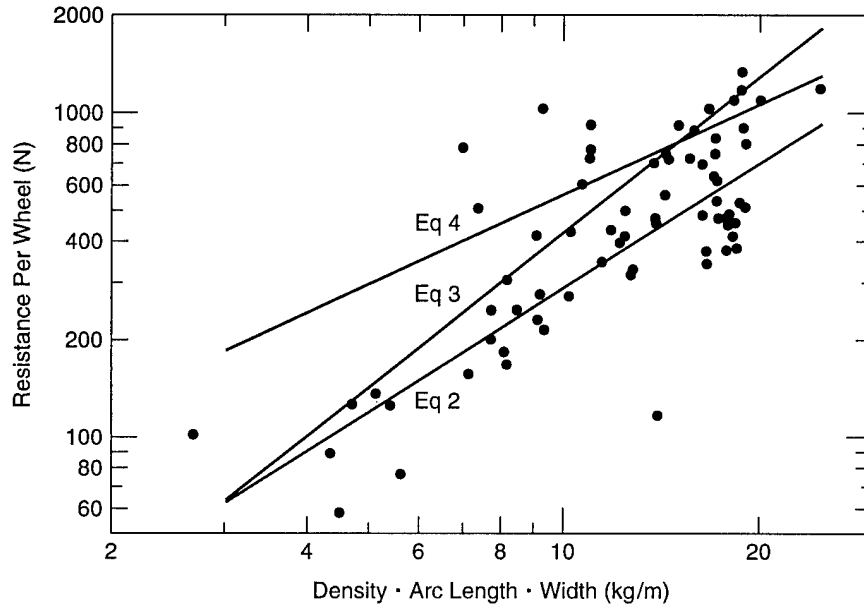
6

Figure 3. Leading tire motion resistance.

eq 3. Further analysis of this data set (old and new CIV data) using a stepwise regression procedure showed that an equation including only snow depth and the ratio of arc length a to $1/4$ the perimeter of the wheel provided a slightly better correlation to the data. This equation

$$R_s = 66.148 + 51.915h - 490.26\left(\frac{4a}{r\pi}\right) \qquad (6)$$

has an r^2 of 0.68. It is interesting that neither the wheel width nor snow density is included in the equation, even though wheel width varied from 0.156 to 0.274 m (albeit there are only a few data points at the narrowest width). The lack of a wheel width effect was also suggested by the analysis of snow deformation by a wheel presented in Ap-

pendix B. Snow density (i.e., snow characteristics other than depth) may have been too similar between tests to develop a clear effect.

Trailing tire resistance

The initial analysis consisted of examining scatter plots of the independent variables (snow depth, density, tire width, sinkage and velocity) and several different combinations of these parameters vs. several forms of the dependent variable: rear wheel motion resistance (R_r). The following forms of the trailing wheel motion resistance were considered—rear tire motion resistance (R_r), rear tire motion resistance divided by vertical load (R_r/V_r) (coefficient form), ratio of rear tire motion resistance to front tire motion resistance (R_r/R_f), and
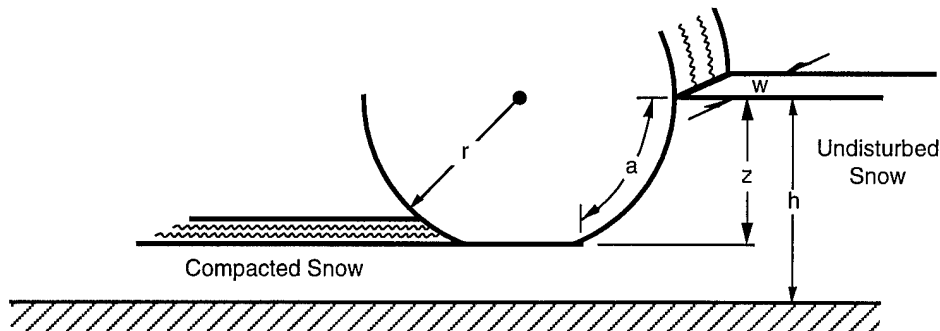

Figure 4. Snow and tire characteristic dimensions.

7

Table 4. Average rear resistance coefficient and standard deviations by data set.

Data set	Number of observations	Avg. resistance coefficient	Standard deviation	Average snow depth (cm)	Average snow density (Mg/m³)
1	4	0.0207	0.0095	15.6	0.165
2	4	0.0171	0.0044	17.6	0.160
3	8	0.0056	0.0036	20.0	0.220
4	12	0.0140	0.0061	22.2	0.220
5	6	0.0728	0.0120	33.8	0.160
6	4	0.0068	0.0039	12.6	0.110
7	6	0.0199	0.0072	15.4	0.110
8	2	0.0152	——	15.8	0.250
9	4	0.0378	0.0168	14.6	0.230

the ratio of rear tire motion resistance to front tire motion resistance in coefficient form $(R_r V_f /R_f V_r)$. This analysis was done set by set and for all of the data combined. No clear dependence was found between any of the variables and any of the rear tire motion resistance "parameters."

It was next hypothesized that the rear tire motion resistance coefficient (R_r /V_r) may be a constant (at least for the CIV) under similar test conditions. To investigate this hypothesis, the average and standard deviation for each data set were calculated (Table 4); those sets that were collected

under clearly different conditions were not included in the analysis. Data set 5, which clearly has a higher resistance coefficient, was neglected since it was obtained in snow that was much deeper than that in the other data sets. Data sets 6 and 8 were obtained by towing the CIV in the ruts that were made by the tow vehicle, thus the trailing tire data are actually the fourth pass over the snow cover.

Inspection of the remaining data sets (1, 2, 3, 4, 7 and 9) showed that the average values of the highest (set 9) and lowest (set 3) didn't seem to
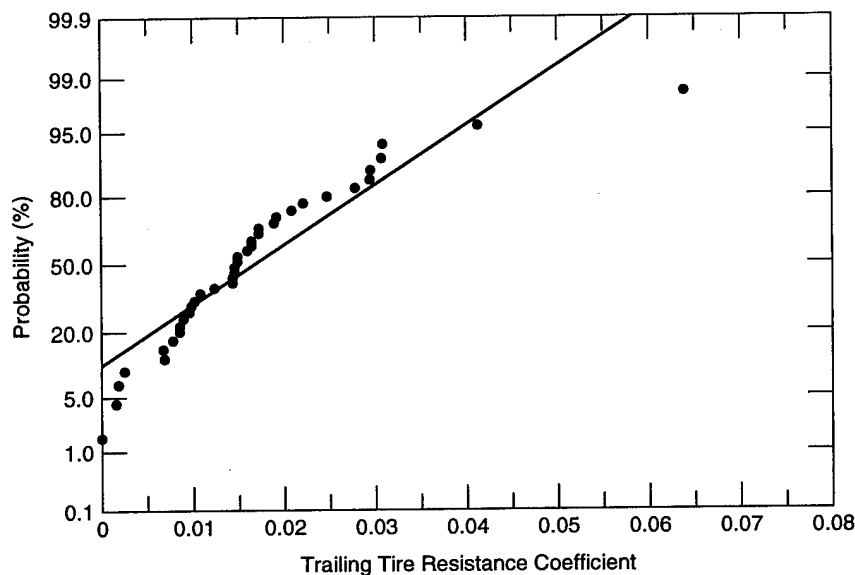

Figure 5. Normal probability plot.

Table 5. Analysis of variance.

Data set	Number of observations	Mean
1	4	0.0207
2	4	0.0171
3	8	0.0056
4	12	0.0140
7	6	0.0199
9	4	0.0378
Total	38	

For all data sets

	SS	df	MS	F
TOTAL	0.016013	38		
CF	0.01059	1		
TR	0.002986	5	0.000572	
RES	0.002437	32	0.0000761	7.516

Since $F_{0.95}$ (5,32) = 2.5, there is a difference between data sets.

For data sets 1,2,3,4 and 7

	SS	df	MS	F
TOTAL	0.009175	34		
CF	0.0002698	1		
TR	0.0075927	4	0.001898	
RES	0.0013125	29	0.000045286	41.92

Since $F_{0.95}(4,29)$ = 2.7, there is a difference between data sets.

For data sets 1,2,4 and 7

	SS	df	MS	F
TOTAL	0.008817	26		
CF	0.007399	1		
TR	0.0002128	3	0.00007093	
RES	0.001205	22	0.00005479	1.295

Since $F_{0.95}(3,22)$ = 3.05, there is no difference between data sets.

agree with the other data (Table 4). There was no apparent reason for this on the basis of test conditions or procedure, although data set 9 may have been collected in hard "crusty" snow. To legitimately combine these data sets, the data need to be random and normally distributed and the variances need to be homogeneous. Once this is shown, an analysis of variance (ANOVA) test or multiple range test can be used to determine if the data sets can be combined.

Figure 5 is a normal probability plot of data sets 1, 2, 3, 4, 7 and 9. The data fell on nearly a straight line, indicating that they are random and normally distributed. Bartlett's test for homogeneity of the error variance showed that the variances were not different at the 95% confidence level. A multiple range test indicated that sets 3 and 9 should not be included, and Table 5 contains the results of a series of ANOVA tests to determine which of the data could be combined.

Between each ANOVA test, a procedure following Grubbs (1969) was used to determine if the extreme values could be considered outlying observations. This analysis also showed that sets 3 and 9 can be dropped from further analysis on the basis of statistical arguments. The average rear tire motion resistance coefficient R_r/V_r of the remaining data sets is 0.0169 with a 95% confidence interval of 0.0138 to 0.0199. These values are shown graphically on Figure 6. It should be noted that if both sets 3 and 9 are included, the average R_r/V_r is 0.0167 with a confidence interval of 0.0127 to 0.0207, which really isn't much different from the values obtained from the four data sets, although it is serendipitous that the effects of these two tests (3 and 9) average each other out.

From the above analysis, it appears that a trailing tire in dry snow that is less than 0.22 m deep and that has a density less than about 0.250 Mg/m^3 will have a resistance coefficient of about 0.017, although values as low as 0.0 and as high as 0.64 were measured. No data were obtained for snow densities greater than 0.250 Mg/m^3. It should also be noted that the rear wheels of the CIV carry less weight than the front wheels, and the effect of a trailing tire carrying a higher weight is not known.

Deep snow

Tests 0125f–0125i (data set 5) were done in relatively deep snow compared to the other tests. These deep snow tests resulted in limited data for two different trailing tire configurations. Data were obtained similar to those described above (all four wheels of the CIV rolling freely in undisturbed snow) and with the front wheels driving while the rear wheels were rolling free. This second condition, freely rolling wheel trailing a *driven* tire, is significantly different from that described earlier.

To tow the CIV through this deep (36 cm) snow, a packed path was first made for the lead vehicle. Additionally, the snow was deep enough such that the undercarriage of the lead vehicle disturbed the snow in which the right side wheels of the CIV traveled. Thus, in Table 3, for tests 0125f and 0125g, data are only presented for the left side
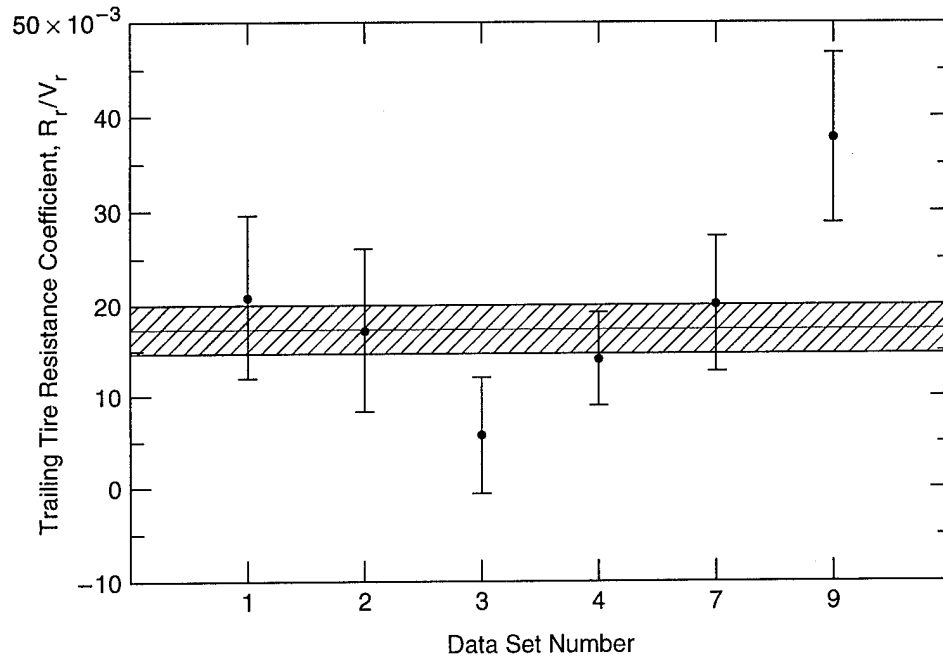
Figure 6. Ninety-five percent confidence intervals for the means. Shaded area is the mean and 95% confidence interval for combined sets 1, 2, 4 and 7.
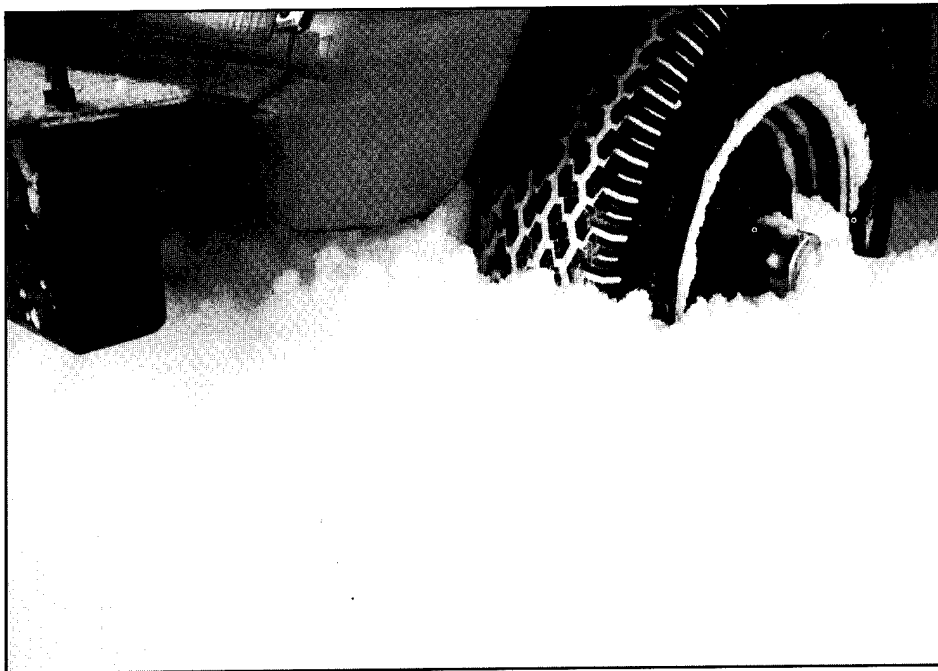

Figure 7. Snow in front of wheel.

Figure 8. CIV in deep snow.

of the CIV. The snow in these tests was about 36 cm deep, which is about equal to the undeflected radius of the tires. Figure 7 shows how the snow piled up in front of a wheel, although it is not clear whether this snow came from under the vehicle or was pushed up from the area in front of the tire (note the "bow wave" in front of the CIV in Fig. 8).

Because of the difficulty of towing the CIV in snow this deep, it was disconnected from the tow vehicle and driven in front-wheel drive. It became immobilized when the snow piled up in front of the bumper (Fig. 8), so that tire chains had to be installed on the front wheels. This, and slightly shallower snow in the succeeding area, allowed some data to be collected. Tests 0125h and 0125i yielded trailing tire resistance behind a driven tire. The trailing tire resistance coefficients were 0.064, 0.057, 0.064 and 0.077 for the left and right sides of tests 0125h and 0125i respectively. These values and those of tests 0125f and 0125g are much higher than those measured in the other tests; this is most likely attributable to snow falling back into the rut behind the front wheels in deep snow, or in the case of tests 0125h and 0125i, attributable to the disruption of the packed snow rut by a preceding driven tire. (A preceding driven tire disrupts the snow through the effects of wheel slip; compared to the effects of a freely rolling wheel, the snow in the bottom of the rut is made uneven and looser.)

Blaisdell (1987) measured trailing tire resistance using the CIV with load cells mounted only on the front axle. He used two different indirect methods to accomplish this. In one procedure, he drove the front wheels at a steady speed and assumed that the measured force on the front load cells was equal to the trailing tire resistance (the measured forces for the CIV are analyzed below). A comparison of these measurements are made with those of tests 0125h and 0125i in Figure 9, which shows all the values falling in the same range.

To see if the rear coefficients were related to the slip of a preceding driven wheel, the leading tire's Differential Interface Velocity (DIV) was compared with the trailing tire resistance coefficients. There did not appear to be any clear cause and effect.

Undercarriage drag

Figure 10 shows a force balance on the entire vehicle (neglecting air resistance); once the vehicle is moving at a steady speed, the sum of forces should be zero. If the CIV is driven at a steady speed, the load cells on the driven axles measure the resistance to motion felt by the rest of the vehicle (i.e., the net traction measured by these load cells must equal the sum of all the other resistances). Since some of the CIV undercarriage was dragging in the deep snow tests, undercarriage drag can be estimated. Minimum ground clearance for the CIV is 14.0 cm for the torsion bar brackets and 19.1 cm for the front differential, and

11

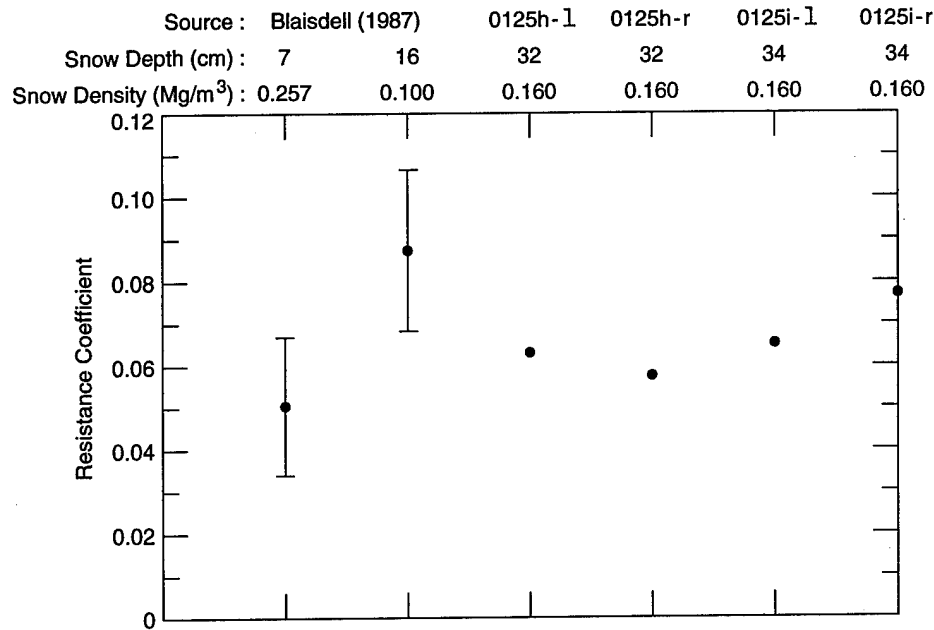| Source :	Blaisdell (1987)		0125h-l	0125h-r	0125i-l	0125i-r
Snow Depth (cm) :	7	16	32	32	34	34
Snow Density (Mg/m^3) :	0.257	0.100	0.160	0.160	0.160	0.160

Figure 9. Comparison of values measured by Blaisdell (1987) and those obtained here for trailing tire resistance behind a driven wheel. Blaisdell's data are shown ± 1 standard deviation.

vehicle sinkage was about 28 cm in the deep snow. Table 6 is a summary of the forces on the CIV; hard surface resistance was estimated using equations developed by Shoop (1992) for the left and right front tires of the CIV based on velocity. Since no data are available on the hard surface resistance of the rear CIV tires, it was assumed to be the same as the front. From Figure 10, the sum of the measured forces should equal the force ascribable to the dragging undercarriage, if the momentum effect can be assumed to be zero (i.e., the vehicle is not accelerating or decelerating). Figure 11 gives plots

of the sum of the load cell output, reading by reading, and the corresponding velocity. It does not appear that momentum has an effect, since the velocities are nearly steady, and the small variations in velocity don't necessarily correspond to changes in the sum of the forces on the vehicle.

The force exerted on the undercarriage is estimated to be 734 and 770 N for tests 0125h and 0125i respectively. It can be seen that, without including the effect of the slope, the vehicle would have been immobilized. Using the information from tests 0215f and 0215g to obtain a value of resistance
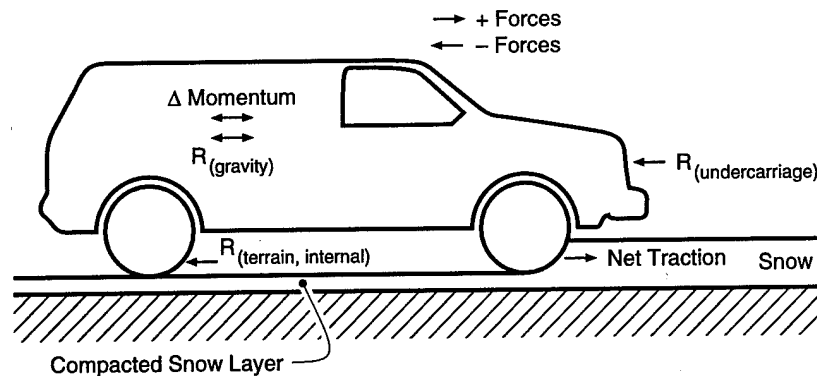

Figure 10. Forces acting on CIV (front wheel drive). Net traction + R(terrain, internal) + R(gravity)* + Δmomentum + R(undercarriage) = 0.

---

*Horizontal component of gravitational force used when operating on a slope.

12

Table 6. Analysis of undercarriage drag, tests 0125h and 0125i.

	Test 0125h	Test 0125i
Total average vertical force	25,371 N	25,280 N
Longitudinal forces[a]:		
Average left front	454.6	492.7
Average right front	634.0	771.0
Average left rear	–368.3	–368.3
Average right rear	–347.8	–456.4
Hard surface resistance[b]	–507.4	–505.6
Net force (available) w/o gravity	–134.9[c]	–66.6
Average force due to gravity[d]	869	837
Net force available with gravity[e]	734	770.4

[a]From Table 3.
[b]Estimated using an average coefficient of 0.02.
[c]A negative value infers that the vehicle would be immobilized (no tractive reserve).
[d]The CIV tilt sensor measured an average angle (ϕ) of –1.96 and –1.89°, indicating that the CIV was moving downhill. The force due to gravity was calculated by multiplying the total average vertical force by sin ϕ.
[e]Since the vehicle was assumed to be traveling at a steady speed, this value must be attributed to undercarriage drag.

attributable to the four wheels and the average undercarriage resistance results in an undercarriage resistance that is 22% of the total vehicle resistance or 1.14 times R_s. This is interesting in that Richmond et al. (in prep) use a multiplier of 1.25 to estimate undercarriage drag for this condition.

Multiple passes

Data sets 6 and 8 were obtained by towing the CIV such that the wheels traveled through the ruts created by the tow vehicle. The forces measured may be assumed to be estimates of third and fourth trailing tires. It was further assumed that tests 0126g–0126i could represent the first and second wheels; together, these data represent a complete set of resistance data for axles 1 through 4 (Table 7). Tests 0202f–0202h were analyzed similarly.

Comparing the average resistance coefficients between the two data sets shows that the resistance data measured during the 0202 tests (snow depth 15.8 cm with a density of 250 kg/m³) are much higher than the data from the 0126 tests (snow depth 12.6 cm with a density of 110 kg/m³).

This is most likely caused by snow falling back into the rut, which is common for deep snow covers (Fig. 12) and may have happened in this test. Unfortunately, this effect was not identified early enough during the testing to be fully investigated. These data are shown graphically in Figure 13. The data of test 0126 seem to agree well with the theory that succeeding tires should have decreasing resistance, the average values for the third and fourth "axles" being 0.0094 and 0.00685 respectively.

The implication of this analysis is that, for vehicles with more than two axles such as the HEMTT and LAV, a rationale needs to be determined for modeling these additional trailing tires. It does not appear that individual wheel resistance on large vehicles will be directly measurable in the near future.

SHALLOW SNOW RESISTANCE MODEL

As mention earlier, Richmond et al. (1990) analyzed resistance data from a large number of tests and vehicles, obtaining eq 4 from data for both wheeled and tracked vehicles. Richmond (1990) combined the data into groups of like vehicles and developed a set of equations of the same form as eq 4, but no significant improvement in the correlation coefficients resulted. In these earlier analyses, only the data from the CIV could be considered as leading wheel data. The data obtained from the other vehicles were "whole" vehicle resistances (from snow) values. To try and reduce the data to fit one equation, the whole vehicle resistance was simply divided by the number of wheels for each vehicle.

Appendix B contains a discussion of the deformation of snow by a wheel and concludes along with eq 6 that wheel width may not be as an important parameter as arc length and initial density. Additionally, the ratio of wheel radius to sinkage should be considered to account for increased deformation (more bulldozing) in deeper snow covers, possibly in the form ($4a/r\pi$) noted earlier. With these ideas in mind, and with the new trailing tire information, an attempt was made to improve the currently used algorithm (eq 4 and 1) for predicting motion resistance for wheeled vehicles in snow.

After several attempts were made to extend the CIV trailing tire data to the HMMWV data, without any clear success, the motion resistance data base obtained during the Wheels vs. Tracks shallow snow tests was reexamined. Appendix C con-

13
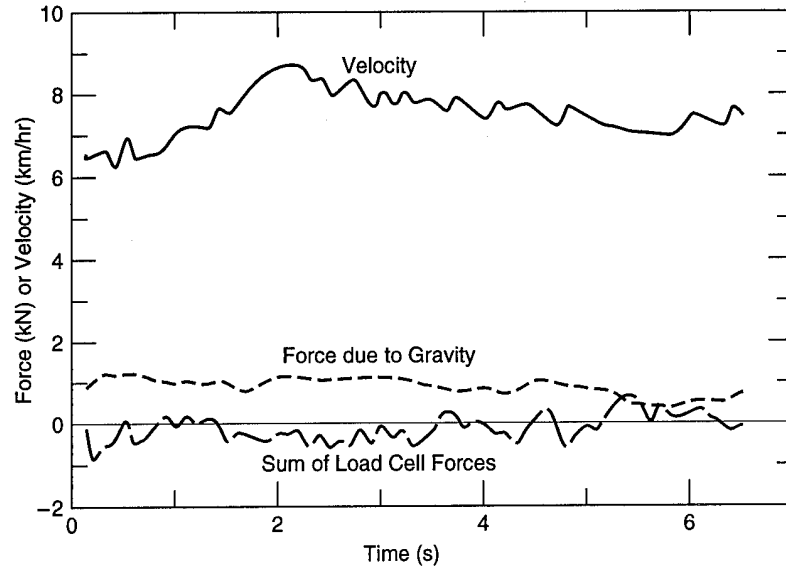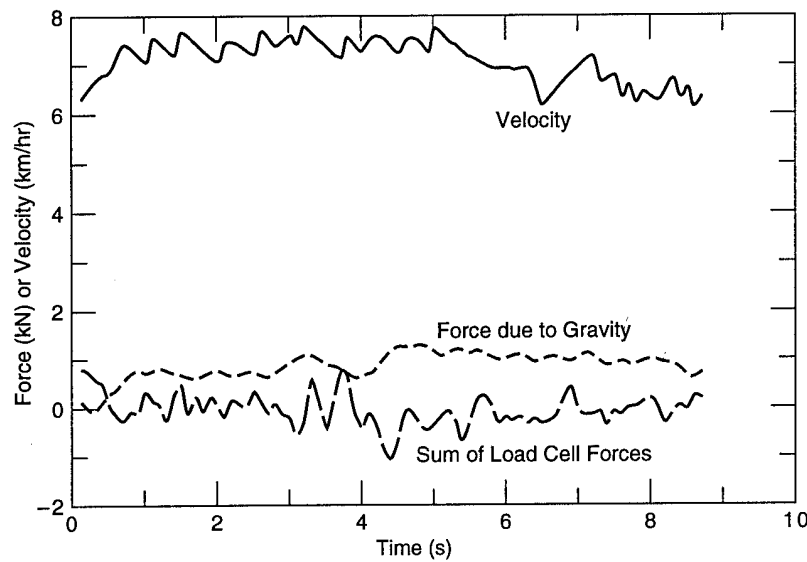
a. Test 0125h.

b. Test 0125i.

Figure 11. Net force and velocity vs. time.

tains the data presented by Blaisdell et al. (1990), Richmond et al. (1990), and Green and Blaisdell (1991), combined with the data presented herein. The data are presented in the form in which they were used to develop the following algorithms.

The first step was to reevaluate the sinkage relationship of Richmond et al. (1990). It was found that, if the tracked vehicle data were ignored, a linear trend exists between the highest contact pressure of a preceding wheel and the theoretical

final density (ρ_f). The sinkage prediction algorithm for undisturbed snow remains as (eq 1)

$$z = h\left(1 - \frac{\rho_0}{\rho_f}\right)$$

and the final density is now calculated using

$$\rho_f = 0.519 + 0.0023 p_{max} \tag{7}$$

14

Table 7. Multiple axle analysis of resistance, tests 0126 and 0202.

Test no.	Snow depth (cm)	Density (Mg/m³)	Force (N) 1*	2	3	4	Coefficient (R/V) 1	2	3	4
0126e-l	12.2	0.11	——	——	54.3	46.7	——	——	0.0079	0.0088
0126e-r	11.2	0.11	——	——	93.0	3.1	——	——	0.0136	0.0006
0126f-l	14.2	0.11	——	——	74.7	60.5	——	——	0.0107	0.0110
0126f-r	12.8	0.11	——	——	104.1	36.9	——	——	0.0155	0.0070
0126g-l	13.6	0.11	167.7	85.0	——	——	0.0241	0.0163	——	——
0126g-r	12.7	0.11	182.8	79.6	——	——	0.0265	0.0145	——	——
Average	12.7	0.11	175.3	82.3	81.5	36.8	0.0253	0.0154	0.0094	0.0069
0202f-l	18.5	0.25	——	——	657.0	167.3	——	——	0.1002	0.0304
0202f-r	13.2	0.25	——	——	311.8	0.0	——	——	0.0415	0.0000
0202g-l	16.1	0.23	876.7	111.2	——	——	0.1271	0.0207	——	——
0202g-r	12.8	0.23	521.3	138.3	——	——	0.0724	0.0247	——	——
0202h-l	18.6	0.23	831.8	327.4	——	——	0.1187	0.0638	——	——
0202h-r	10.8	0.23	435.0	240.2	——	——	0.604	0.0411	——	——
Average	15	0.23	666.2	204.3	484.4	83.7	0.0955	0.0376	0.0709	0.0152

*Axle number.

where p_{max} is the maximum contact pressure of the wheels in kilopascals. Figure 14 is a comparison of the two prediction methods. Much better agreement is obtained using eq 1 and 7 as compared to eq 1 and the table of values for ρ_f.

Using the resistance data in Appendix C and a nonlinear regression analysis combined with the assumptions that 1) the resistance of the first wheel through undisturbed snow is a function similar to eq 4 and 2) that the resistance of trailing tires can be
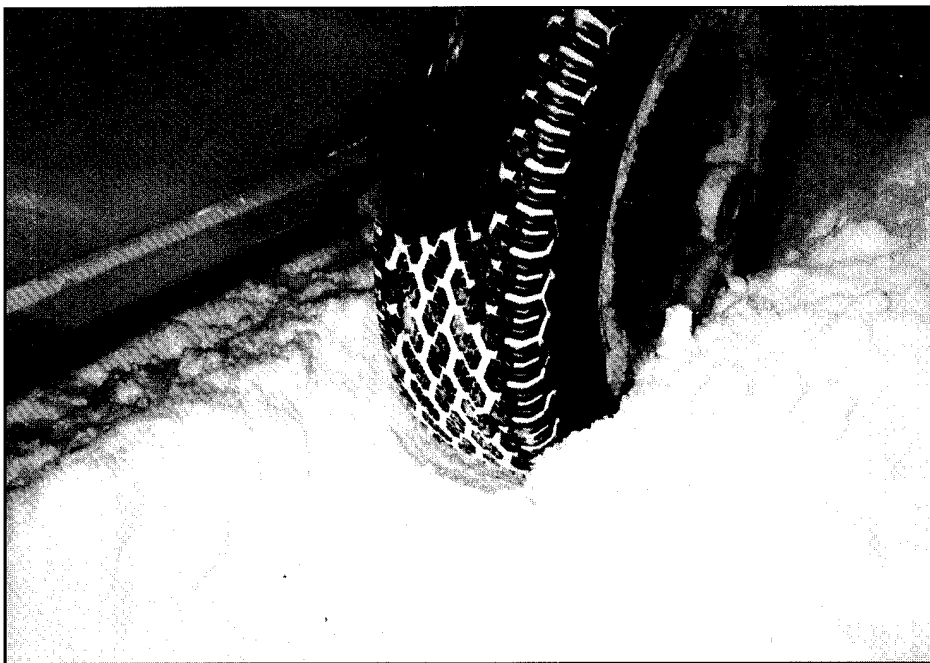

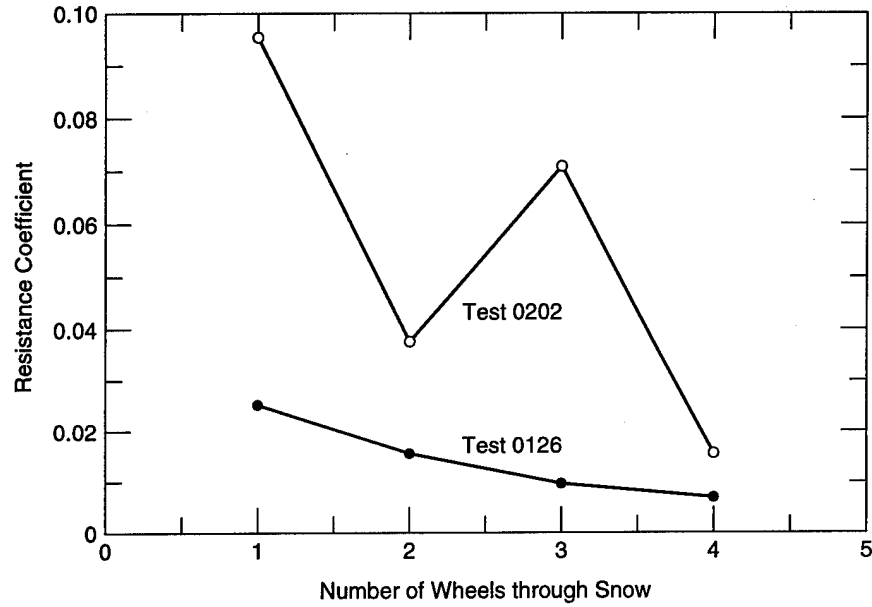Figure 12. Loose snow in rut in front of trailing tire.

Figure 13. Plot of resistance coefficients for multiple passes.

represented as a coefficient multiplied by the vehicle wheel load, and 3) using the sinkage prediction algorithm of eq 1 and 7, resulted in the following equation for 1/2 the total vehicle resistance (each axle is considered to be symmetrical).

$$R_s = 13.6041(\rho_o wa)^{1.26} +$$

$$0.0475\,h_r\,L_2 + 0.0246\,h_r\,L_3 \tag{8}$$

where
$$h_r = 1.0 \text{ if } h \le 0.22\text{ m}$$

$$h_r = \frac{h}{0.22} \text{ if } h > 0.22\text{ m}$$

where
h = snow depth (m)
L_2 = 1/2 the load (N) on the second axle
L_3 = 1/2 the load (N) on the third axle.

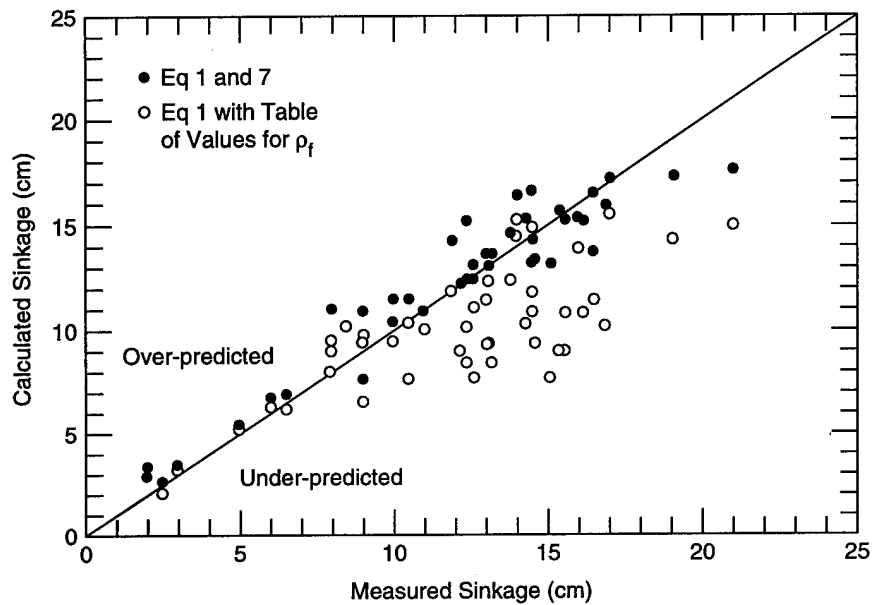*Figure 14. Comparison of two sinkage prediction algorithms.*

16

a. Using eq 1, 7 and 8.　　　　　　　*b. Using eq 4 and 1 with tabular values of ρ_f.*
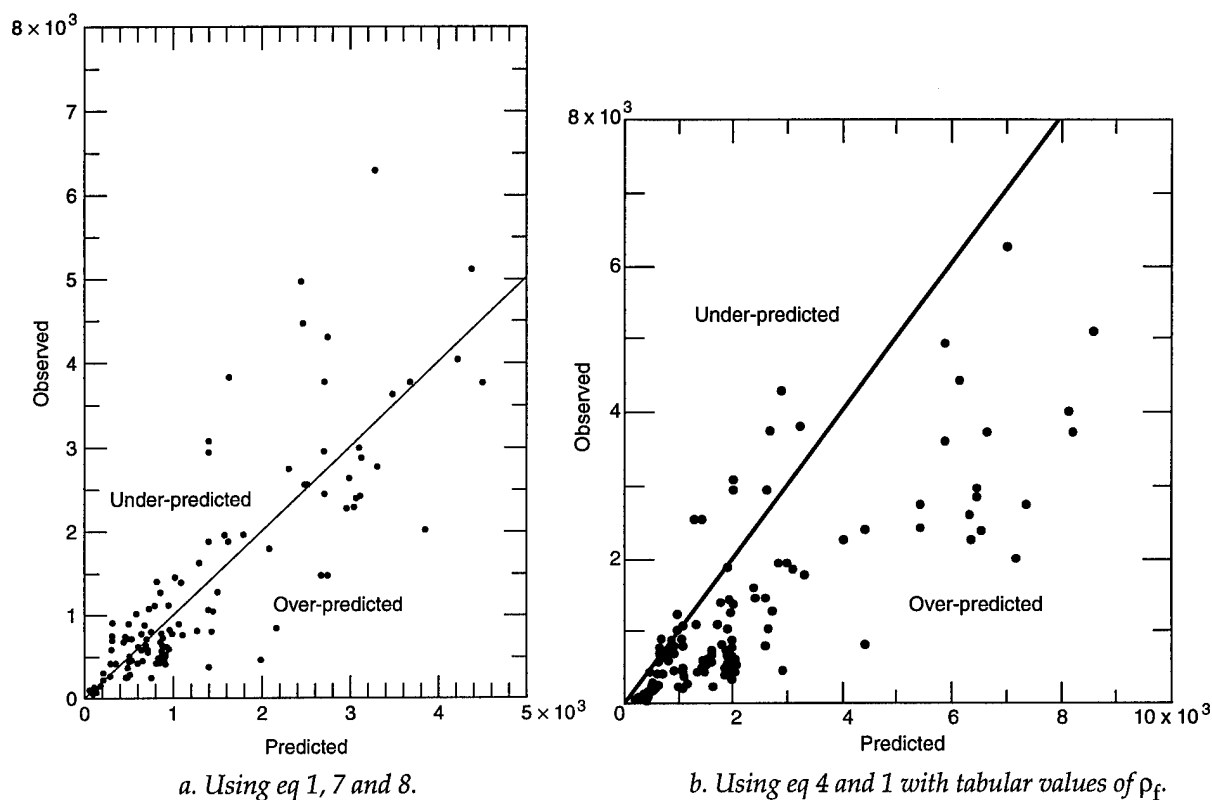
Figure 15. Comparison of predicted and measured resistance values.

The term ($\rho_0 wa$) is in kilograms per meter. It is interesting to note that adding a term for the fourth axle adds little to the accuracy of the equation and forces the coefficient for the third axle to be negative, a physical impossibility. The rationale for the ratio of snow depth to the depth of 0.22 m is to account for the effect of snow falling back into a rut behind a leading wheel in deep snow. The trailing tire coefficients obtained are higher than anticipated, and this is thought to be attributable to higher loads on the trailing axles for most of the vehicles in the data base, as compared to the CIV, which has less weight on the trailing axle.

Other forms of the term ($\rho_0 wa$) were investigated using the ideas presented earlier; little or no improvement was found in the regression analysis. Figure 15 shows a comparison of the predicted vs. measured resistance. It can clearly be seen that eq 8 produces excellent results and a marked improvement over earlier algorithms. Table C1 contains the actual predictions and residuals.

SUMMARY

Several aspects of the interaction between snow and a wheeled vehicle were investigated. The resistance of a trailing wheel can be considered a constant in most cases; however, snow falling back into the rut behind a leading wheel results in higher values and seems to be related to initial snow depth. The true effect of wheel width on resistance of a leading wheel is still not known and should be studied using a numerical technique where other parameters can be held constant. Limited data were presented for undercarriage drag, and since this will be the primary cause of immobilization on level surfaces, it deserves further investigation.

A new and significantly improved algorithm for predicting sinkage and motion resistance in undisturbed snow was presented. This improved algorithm should be implemented in current cold regions mobility models.

LITERATURE CITED

Blaisdell, G.L. (1983) The CRREL instrumented vehicle: Hardware and software. USA Cold Regions Research and Engineering Laboratory, Special Report 83-3.

Blaisdell, G.L. (1987) Trailing-tire motion resistance in shallow snow. *Proceedings of the 9th Inter-*

national ISTVS Conference, Barcelona, Spain, p. 296–304.

Blaisdell, G.L., P.W. Richmond, S.A. Shoop, C.E. Green and R.G. Alger (1990) Wheels and tracks in snow: Validation study of the CRREL shallow snow mobility model. USA Cold Regions Research and Engineering Laboratory, CRREL Report 90-9.

Green, C.E. and G.L. Blaisdell (1991) U.S. Army wheeled versus tracked vehicle mobility performance test program. Report 2: Mobility in shallow snow. U.S. Army Waterways Experiment Station, Technical Report GL-91-7.

Grubbs, F.E. (1969) Procedures for detecting outlying observations in samples. *Technometrics,* **11**(1): 1–21.

Richmond, P.W. (1990) Vehicle motion resistance due to snow. *Proceedings of the 1990 Army Science Conference.*

Richmond, P.W., G.L. Blaisdell and C.E. Green (1990) Wheels and tracks in snow: Second validation study of the CRREL shallow snow mobility model. USA Cold Regions Research and Engineering Laboratory, CRREL Report 90-13.

Richmond, P.W., S.A. Shoop and G.L. Blaisdell (in prep.) Cold regions mobility models. USA Cold Regions Research and Engineering Laboratory, CRREL Report.

Shapiro, L.H., J.B. Johnson, M. Sturm and G.L. Blaisdell (in prep.) Snow mechanics: Review of the state of knowledge and applications. USA Cold Regions Research and Engineering Laboratory, CRREL Report.

Shoop, S.A. (1992) Precision analysis and recommended test procedure for mobility measurements made with an instrumented vehicle. USA Cold Regions Research and Engineering Laboratory, Special Report 92-7.

Shoop, S.A., E. Berliner and S. Decato (1991) An experimental method for vehicle mobility research on freezing/thawing soil. *Proceedings of the 1st Meeting on Winter Mobility.* Santa Barbara, California: Engineering Foundation.

Yong, R.N. and M. Fugue (1977) Performance of snow in confined compression. *Journal of Terramechanics,* **14**(2): 59–82.
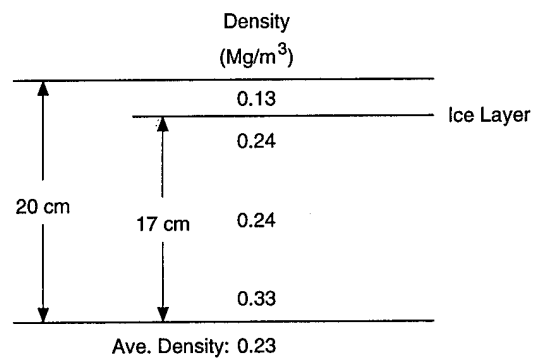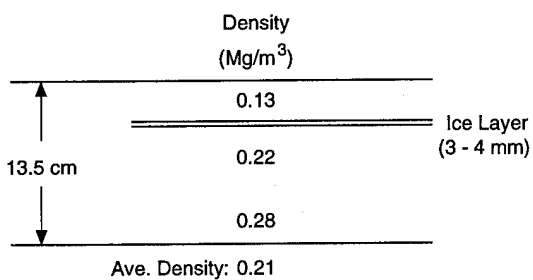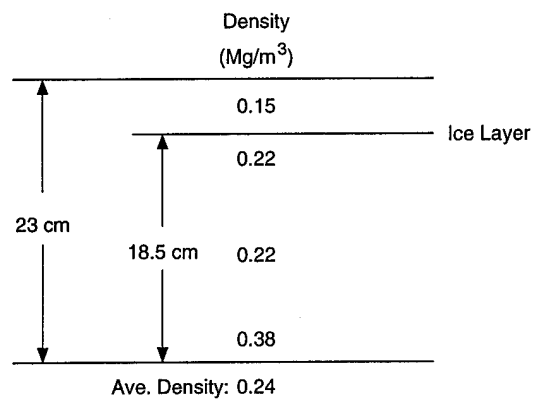
18

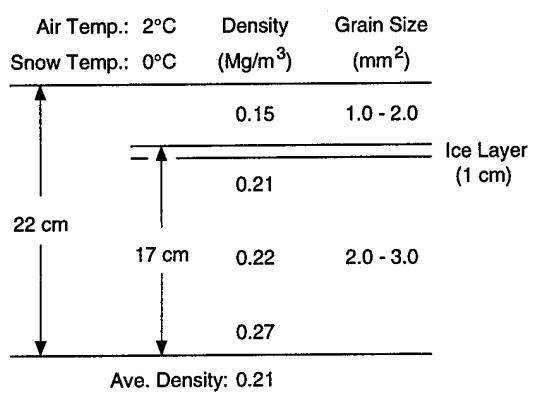# APPENDIX A: SNOW DATA

Tests 0119 H, 0119 O

Density (Mg/m^3)   Air Temp.: −5°C

0.14   Snow Temp.: −6°C

17 cm   Grain Size: 0.5 - 1.0 mm^2

0.20

0.20

Ave. Density: 0.18

Tests 0119 G, 0119 P

Density (Mg/m^3)   Air Temp.: −5°C

0.13   Snow Temp.: −6°C

16 cm   Grain Size: 1.0 - 2.0 mm^2

0.19

0.17

Ave. Density: 0.16

a. 19 January 1993.

Figure A1. Snow data.

Air Temp.: 2°C   Density   Grain Size

Snow Temp.: 0°C   (Mg/m^3)   (mm^2)

```
                    0.15          1.0 - 2.0
                  ─────────────────────────── Ice Layer
                    0.21                       (1 cm)
22 cm     17 cm
                    0.22          2.0 - 3.0

                    0.27
```

Ave. Density: 0.21

Density

(Mg/m^3)

```
                    0.15
                 ─────────────────────── Ice Layer
                    0.22
23 cm    18.5 cm
                    0.22

                    0.38
```

Ave. Density: 0.24

Density

(Mg/m^3)

```
                    0.13
                ═══════════════════ Ice Layer
                    0.22             (3 - 4 mm)
13.5 cm
                    0.28
```

Ave. Density: 0.21

Density

(Mg/m^3)

```
                    0.13
                 ─────────────────────── Ice Layer
                    0.24
20 cm     17 cm
                    0.24

                    0.33
```

Ave. Density: 0.23

b. 22 January 1993.

Figure A1 (cont'd). Snow data.

Air Temp.: −8°C

Density (Mg/m^3)   Temp. (°C)

0.05

1 - 2 mm Flakes

0.14   −5°C   1.0 mm^2 Grains

38 cm

0.21 ——————————————— Ice Layer
0.22   (1 cm)

16 cm   0.24   −3°C   1.0 mm^2 Grains

0.23

Ave. Density: 0.18

Density (Mg/m^3)   Temp. (°C)

0.03

0.06
        −5°C
0.12

37 cm

0.17 ——————————————— Ice Layer
                             (1 cm)
0.22

16 cm   −2°C

0.23

Ave. Density: 0.14

c. 25 January 1993.

Figure A1 (cont'd).

21

Air Temp.: −4°C   Density
Snow Temp.: −4°C   (Mg/m^3)

13 cm

0.09

0.08

0.18

Ave. Density: 0.12

Density

(Mg/m^3)

16.5 cm

0.09

0.08

0.14

Ave. Density: 0.10

d. 26 January 1993.

Air Temp.: 3°C   Density
Snow Temp.: −2°C   (Mg/m^3)

Ice Crust
(1 cm)

0.25   0.20

12 cm

0.24   0.24

Ave. Density: 0.23

e. 2 February 1993.

Figure A1 (cont'd). Snow data.

APPENDIX B: OBSERVATIONS OF SNOW DEFORMATION BY A WHEEL

The purpose of this study was to examine the deformation of snow around a rolling wheel and to identify mechanisms and parameters that could lead to an improved motion resistance model for shallow snow.

Procedure

Deformation experiments were conducted in areas of undisturbed snow that were marked by chalk dust. Holes in the snow, which were punched both perpendicular to and in the direction of vehicle travel, were coated with carpenter's chalk dust. This was done by giving a plastic bottle of chalk dust with a tapered nozzle a quick squeeze into the hole. A 12.5-mm (1/2-in.) diameter dowel was used to punch the holes, which were placed 76.2 mm (3 in.) apart (Fig. B1). After emplacing the dust, a vehicle was driven into the marked area such that the axle passed through the row of perpendicular holes, then the vehicle was backed out. Whenever possible, the wheel was undriven. The snow was then carefully removed to reveal a cross section of the deformed area and the lines formed by the chalk (Fig. B2). Density measurements were made using a 100-cm^3 sampler, which had a 6- by 3-cm cross section. Air and snow temperatures were recorded and, in some cases, so was the grain size.

Three different vehicles were used, although most of the experiments used the CRREL instrumented vehicle. Tire data for each vehicle are in Table B1.

Results and observations

Photographs and documentary data are presented in Figures B3–B5. From these figures it can be seen that, as the wheel rolls forward in the snow pack, deformation occurs in all three directions. In the following discussion, forward is the direction in which the vehicle is moving, perpendicular refers to the direction perpendicular to the direction that the vehicle is moving but parallel to the ground, and downward
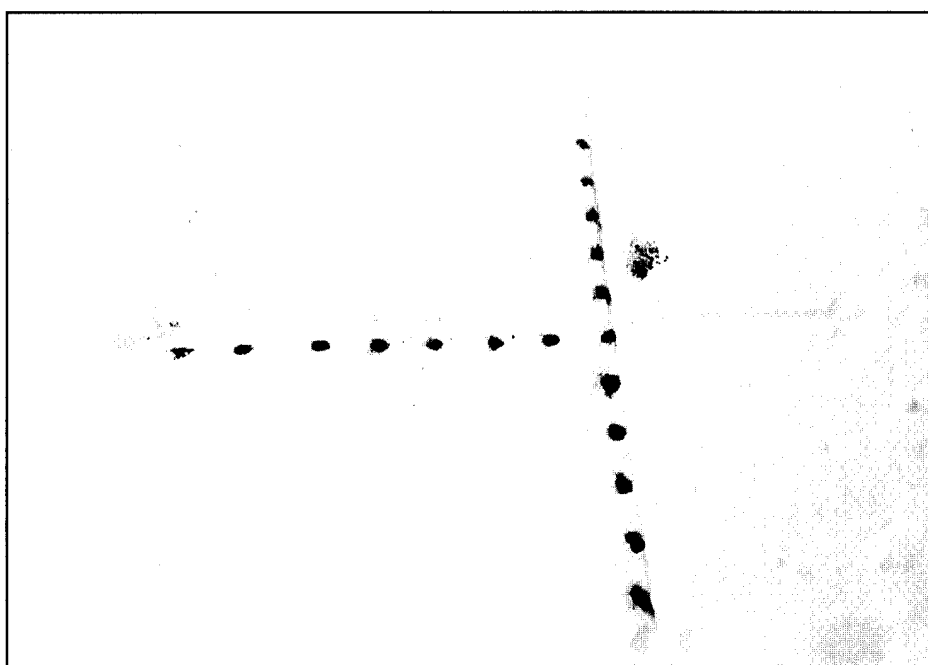

Figure B1. Snow marked with chalk-dust-filled holes.

23

Figure B2. Removing snow to show deformed chalk holes.

or lower infers motion towards the ground. The deformation around a rolling wheel is extremely complex and there seem to be four areas to consider. These are the area under the wheel (the rut area), the area in front of the wheel, and the upper and lower areas adjacent to the wheel sides. The deformation in front of the wheel and to the sides of the wheel in the upper part of the snow cover are related to each other, to the snow depth and the wheel sinkage.

Looking first at the snow under the wheel rut, one can see that the snow at the centerline of the wheel is pushed forward and downward as the wheel rolls forward. Snow that is off the centerline is pushed off at an increasing angle by the compacting snow closer to the centerline. This is seen in the chalk exposed in the area of the wheel rut. The chevron shapes are created because the snow near the center of the snow pack is pushed out further (perpendicularly and forward) than the snow near the snow or ground surfaces. As forward motion continues, the upper snow is pushed downward (see Fig. B3a, c and B4).

Table B1. Vehicle and wheel characteristics.

CRREL Instrumented Vehicle (CIV), 1977 Jeep Cherokee
Tires: Michelin LT 235XCH4, 179 kPa
Radius: 37.5 cm
Maximum deformed width: 26 cm

CRREL Support Truck, 1989 Chevrolet 3/4 ton pickup
Tires: LT 245/75R16 M&S
Radius: 37 cm
Maximum deformed width: not recorded

HEMTT, M997 Heavy Expanded Mobility Tactical Truck
Tires: Michelin 16.0 R20
Radius: not recorded
Maximum deformed width: 48 cm
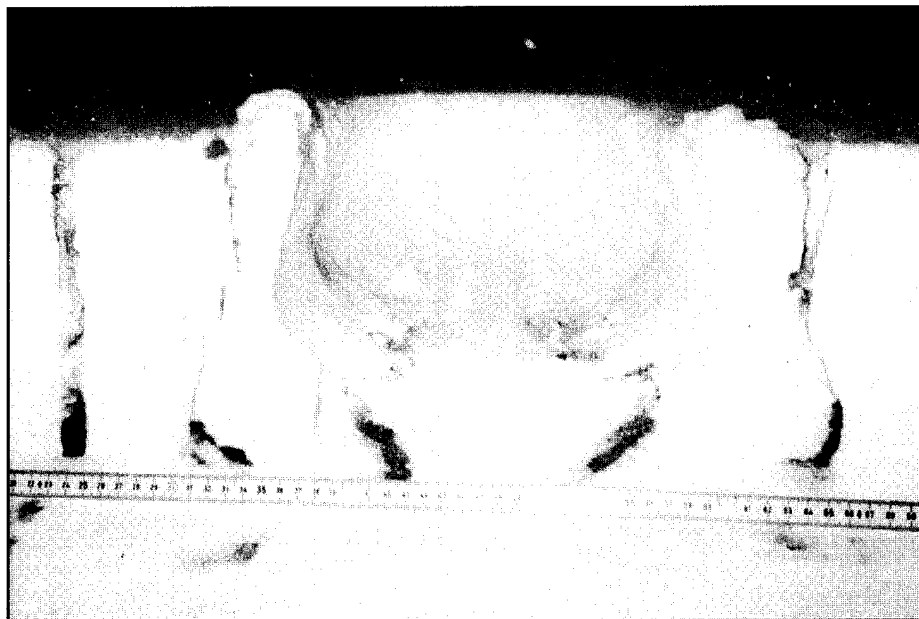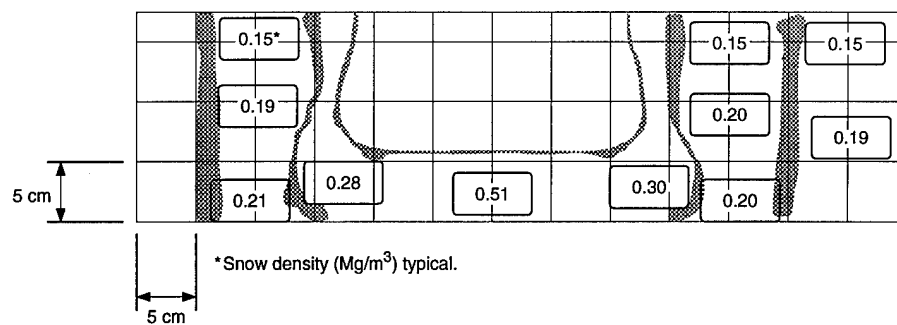
a. 25 January 1992. Snow depth: 19 cm; snow temperature: −10°C; grain size: 0.5–0.75 mm²; air temperature: −8°C; wheel size: LT 235XCH4, 179 kPa; wheel sinkage: 11 cm.

Figure B3. Snow deformation and density distributions.

25

*Snow density (Mg/m³) typical.
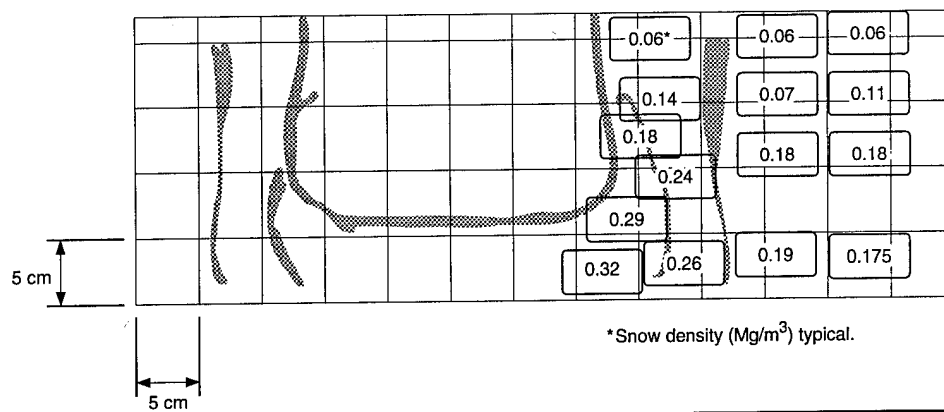
b. 27 January 1992. Snow depth: 21.6 cm; snow temperature: −3°C; grain size: 1.0 mm²; air temperature: −7°C; wheel size: LT 235XCH4, 179 kPa; wheel sinkage: 16 cm.

Figure B3 (cont'd). Snow deformation and density distributions.

Initial Snow
Density (Mg/m^3)

0.11	
0.17	
0.18	
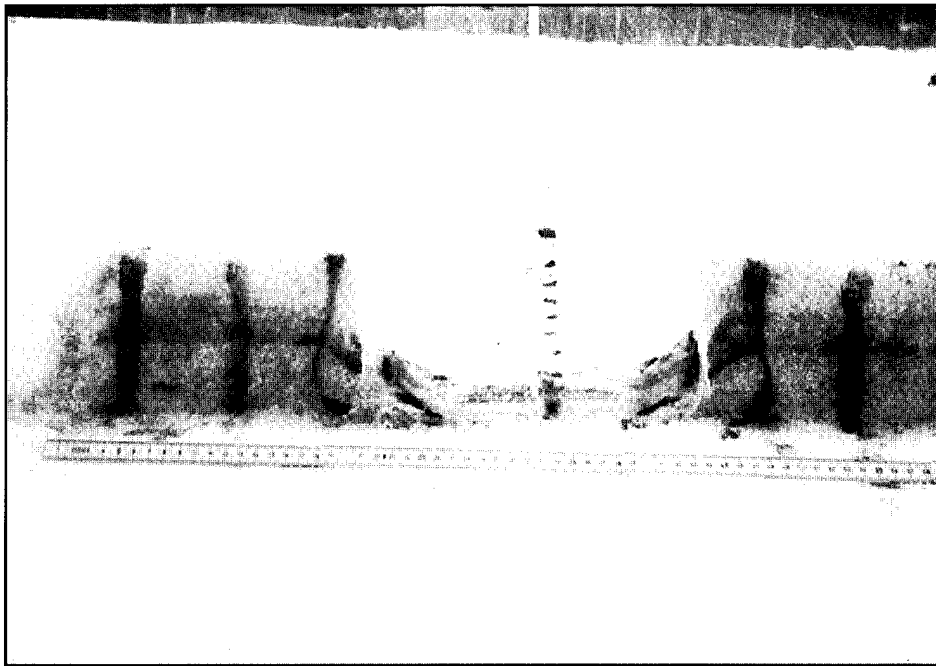
11 cm

c. 29 January 1992. Snow depth: 11.5 cm; snow temperature: –0°C; air temperature: –2°C; wheel size: LT 235XCH4, 179 kPa; wheel sinkage: 8 cm.
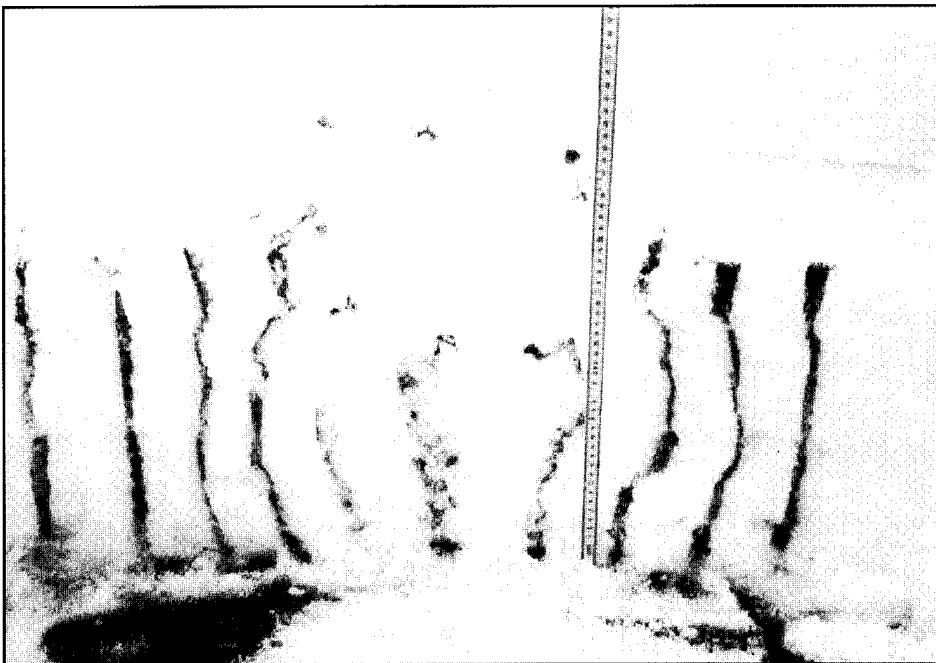
Initial Snow
Density (Mg/m^3)

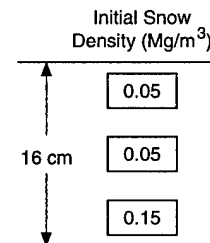| |
|---|
| 0.26 |
| 0.23 |
| 0.27 |
| 0.25 |
| 0.30 |
| 0.27 |

33 cm

d. 3 February 1992. Snow depth: 31.5 cm; snow temperature: –1°C; air temperature: 1°C; wheel size: LT 235XCH4, 179 kPa; snow was removed from the surface so that the wheel could be driven into the deep snow. The axle did not pass the chalk dust holes (4–5 cm short).

Figure B3 (cont'd).

27

Initial Snow
Density (Mg/m^3)

0.20
0.305

0.225

0.25

0.30
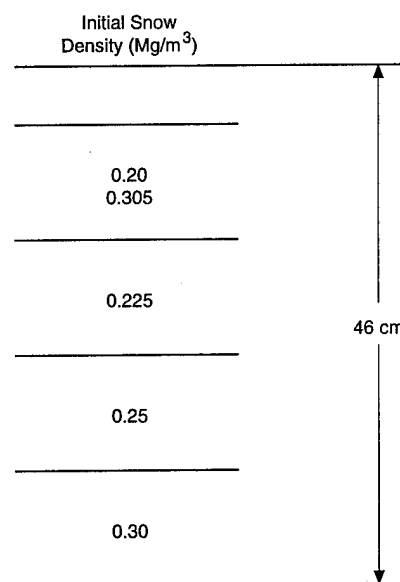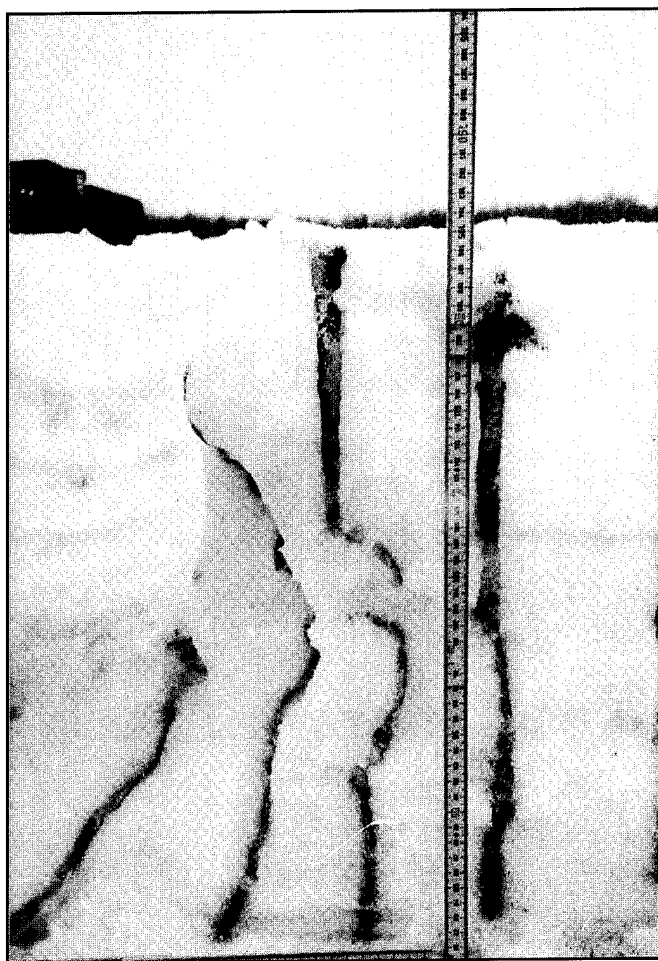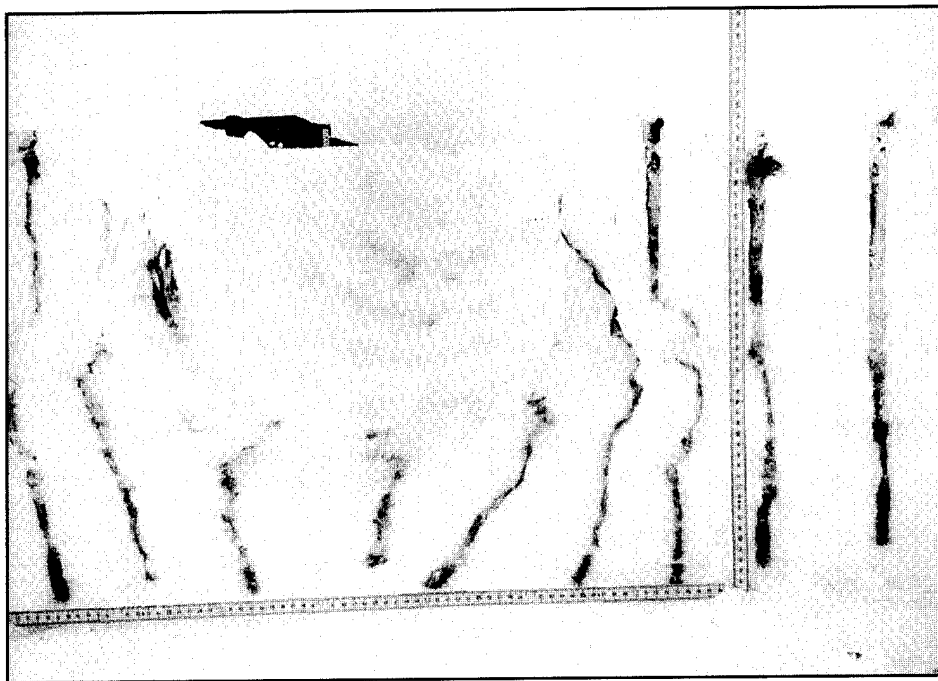
46 cm

e. 4 February 1992. Snow depth: 46 cm; vehicle: HEMTT; wheel sinkage: 24 cm.
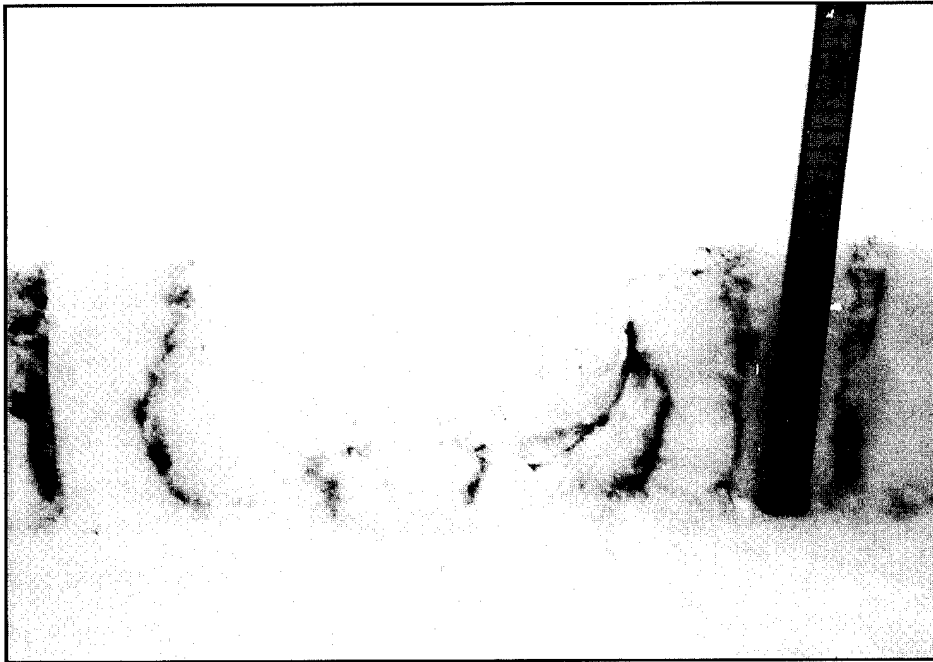
Figure B3 (cont'd). Snow deformation and density distributions.

f. 7 February 1992. Snow depth: 16 cm; snow temperature: −1°C; air temperature: −11°C; wheel size: LT 235XCH4, 179 kPa; wheel sinkage: 10 cm.

Figure B3 (cont'd).

Initial Snow
Density (Mg/m^3)

0.06

0.06

25 cm

0.17
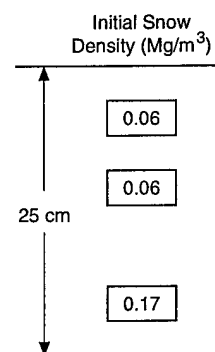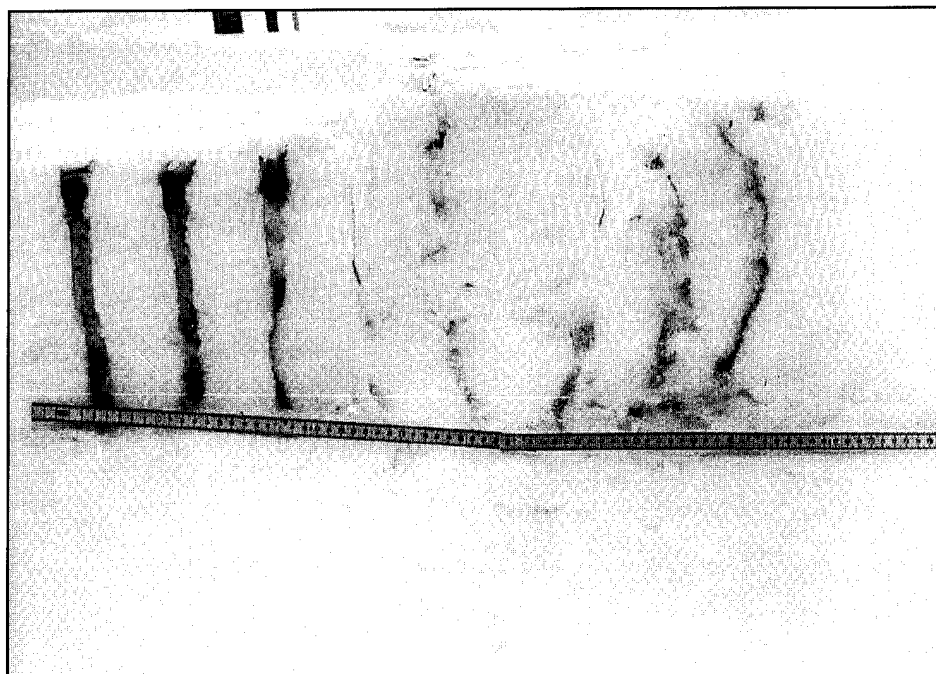
g. 8 February 1992. Snow depth: 25 cm; snow temperature: –13°C; air temperature: –11°C; wheel size: LT 245/ 75 R16, M&S; wheel sinkage: about 14 cm.

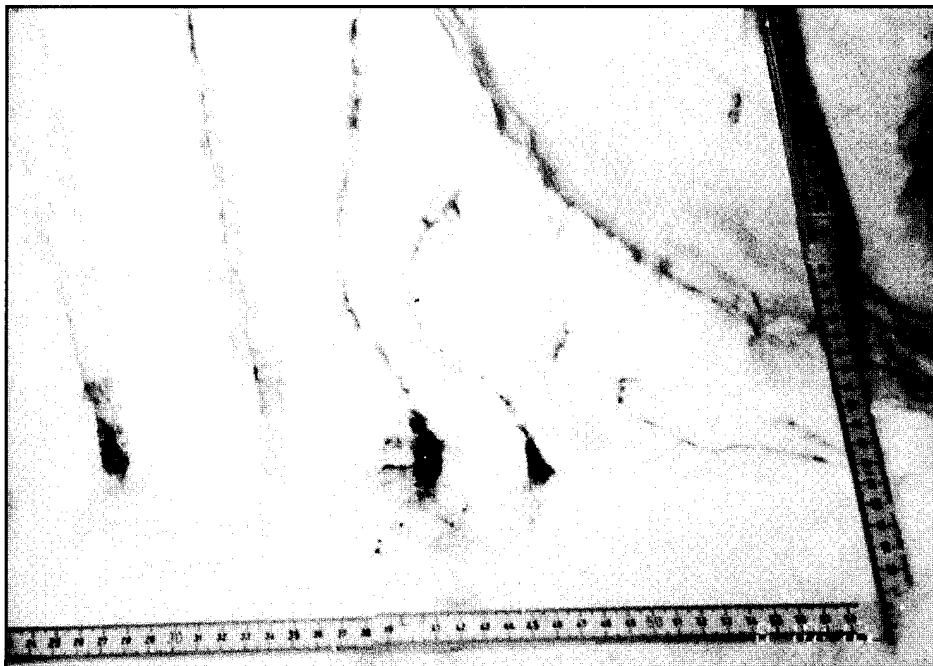*Figure B3 (cont'd). Snow deformation and density distributions.*

Figure B4. Deformation in direction of vehicle travel, same snow properties as in Figure B3f.

For the snow located to the side of the wheel, it appears that the forward displacement component is smaller than the perpendicular displacement, since the chalk at further distances from the centerline has little forward displacement compared to chalk near the wheel (Fig. B3d). This may occur as the full load on the wheel is transferred to the snow, causing additional plastic deformation in the direction perpendicular to the wheel. Maximum deformation seems to occur at or slightly below the bottom of the rut. Additionally, there appears to be little displacement of the snow near the surface compared to snow deeper in the snow cover. This suggests that the strength of the snow lower in the snowpack is more important in resistance calculations.

As wheel sinkage approaches the radius of the wheel, the forward part of the wheel acts more as a bulldozer than a compactor (as in the case of relatively shallow snow) and deformation (both forward and perpendicular) is higher in the snow pack (compare Fig. B3b and c). This is also observed in Figures B4 and B5 for snow deformation in front of the wheel. In shallow snow the deformation area does not extend beyond the leading edge of the tire (Fig. B5), while for deeper snow it does (Fig. B4). This effect can be illustrated by examining the velocity vector components of a rigid, non-slipping wheel. Figure B6 shows the forward, vertical and resultant vectors. One can see how the forward component is reduced as one moves along the tire surface towards the supporting surface.

Most of the experiments were done in relatively low-density snow. When the snow had a higher density, greater deformation was observed (compare Fig. B3b and c). This agrees with observations of soil compaction and suggests that there may be a controlling density (maximum packing density without significant crystal deformation). Recent analysis by Shapiro et al. (in prep.) suggests that intergranular bonding (between snow crystals) is more important than previously suspected, and will greatly control this type of displacement. There is currently no proven method of measuring bond strength and density remains the primary field index of snow strength.
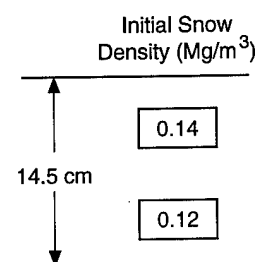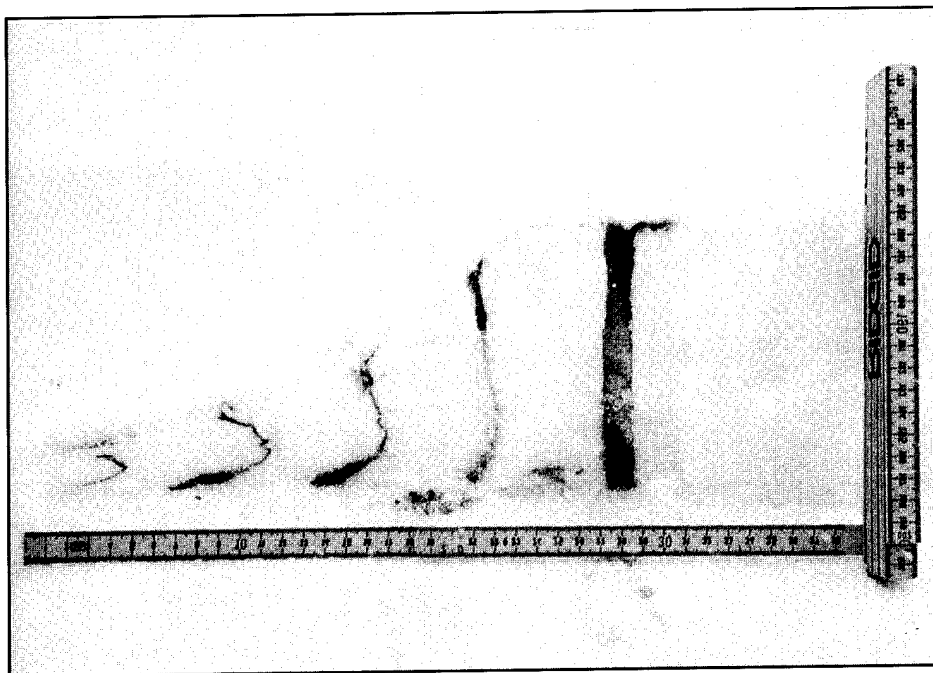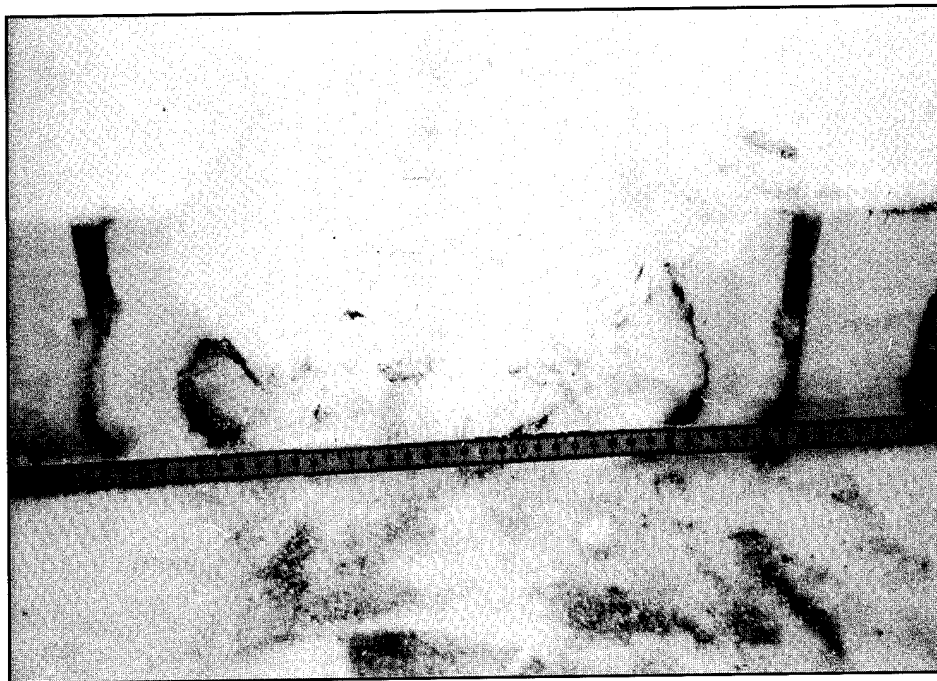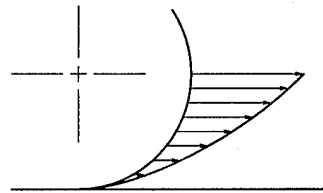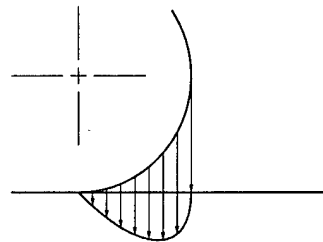
31

Figure B5. Deformation (horizontal and lateral) and initial snow density, 8 February 1992. Snow depth: 14.5 cm; snow temperature: –13°C; air temperature: –11°C; wheel size: LT 245/75 R16, M&S; wheel sinkage: 10.5 cm.

a. Forward component unit vectors.

b. Vertical component unit vectors.
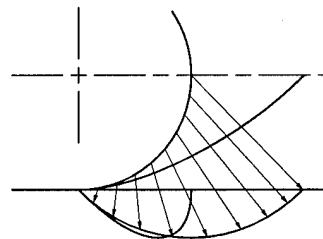
c. Resultant forces.

Figure B6. Forces on a rigid rolling wheel.

Two tests were done in fairly deep snow with significantly different wheels. Figures B3c and d show the results for the CIV wheel (tire width of 26 cm) and the HEMTT (tire width of 48 cm). For both tests the maximum perpendicular displacement is about 18–20 cm. This indicates that the effect of tire width on resistance may not be linear.

Summary

The results of some simple tests to examine the deformation of snow around a rolling wheel were presented. Although they were primarily qualitative, some interesting phenomena were observed. Snow deformation caused by a tire is three-dimensional and, depending on the depth and density, will primarily occur at or below the wheel rut in shallow snow and in the upper area if the snow is deep. Increasing wheel width does not seem to increase deformation in the direction perpendicular to vehicle motion, at least in the one comparison available from these tests. The ratio of wheel radius to sinkage should be considered to account for increased deformation in deeper snow covers.

APPENDIX C: WHEELED VEHICLE MOTION RESISTANCE DATA

Table C1 contains the data for the CIV reported here plus the wheeled vehicle data presented in Blaisdell et al. (1990), Richmond et al. (1990) and Green and Blaisdell (1991). Some corrections were made to the data presented in the earlier reports. The resistance values are presented as the measured value minus the hard surface resistance divided by two, and thus represent the 1/2 of the resistance attributable only to the snow. For each vehicle, normal loads are 1/2 the axle loads; some of the CIV resistance data are for the first axle only and thus it is considered a one-axle vehicle. The sinkage is calculated using eq 1 and 7. The shaded data were not included in the regression analysis for the reasons stated in the Table C1 notes.

Table C1. Wheeled vehicle motion resistance data.

	Depth m	Snow Density kg/m³	Wheel Sinkage m	Wheel Radius m	Wheel Width m	Arc Length m	Meas. Resist N	Normal Load 1st N	Normal Load 2nd N	Normal Load 3rd N	Normal Load 4th N	$a\rho_o w$ kg/m	h_r	Eq (8) Prediction N	Eq (8) Residual N
CIV 1993 Data															
1	0.13	160	0.11	0.37	0.27	0.29	423.91	6931	5424		0	12.45	1	583.9	-160.0
2	0.16	160	0.12	0.37	0.27	0.31	463.06	6646	5454		0	13.45	1	618.6	-155.5
3	0.15	170	0.12	0.37	0.27	0.30	476.85	6887	5450		0	13.92	1	634.4	-157.6
4	0.19	170	0.15	0.37	0.27	0.34	722.83	6800	5401		0	15.62	1	690.6	32.2
5	0.16	160	0.13	0.38	0.26	0.33	589.39	7032	5262		0	13.81	1	621.7	-32.3
6	0.17	160	0.14	0.38	0.26	0.33	450.60	6788	5583		0	13.57	1	628.9	-178.3
7	0.18	170	0.15	0.38	0.26	0.35	652.11	7119	5134		0	15.50	1	673.9	-21.7
8	0.19	170	0.16	0.38	0.26	0.35	599.62	6776	5717		0	15.44	1	699.5	-99.8
9	0.21	220	0.16	0.38	0.26	0.36	410.57	7071	5575		0	20.87	1	890.3	-479.8
10	0.21	220	0.16	0.38	0.26	0.36	729.50	6462	5444		0	20.16	1	857.3	-127.8
11	0.20	220	0.15	0.38	0.26	0.35	584.49	7146	5494		0	20.16	1	859.9	-275.4
12	0.21	220	0.16	0.38	0.26	0.36	796.23	6454	5455		0	20.00	1	851.9	-55.7
13	0.20	220	0.15	0.38	0.26	0.35	517.33	6717	5505		0	20.33	1	866.6	-349.3
14	0.21	220	0.16	0.38	0.26	0.36	645.88	6854	5554		0	20	1	856.6	-210.8
15	0.18	220	0.14	0.38	0.26	0.33	490.64	6876	5362		0	19.16	1	816.3	-325.6
16	0.19	220	0.14	0.38	0.26	0.34	693.47	6663	5696		0	19.20	1	833.6	-140.1
17	0.21	220	0.15	0.37	0.27	0.35	524	7265	5846		0	20.71	1	897.1	-373.1
18	0.38	220	0.27	0.37	0.27	0.48	1313.78	6733	5907		0	28.50	1.227	1611.3	-353
19	0.22	220	0.16	0.37	0.27	0.35	618.74	7296	5701		0	21.23	1	910.1	-291.3
20	0.21	220	0.15	0.37	0.27	0.34	516.44	6499	5236		0	20.34	1	854.2	-337.8
21	0.18	220	0.13	0.37	0.27	0.32	424.36	7071	5648		0	18.91	1	820.7	-396.4
22	0.18	220	0.13	0.37	0.27	0.32	431.92	6730	5315		0	18.85	1	802.8	-370.9
23	0.20	220	0.15	0.37	0.27	0.34	528.45	7058	5627		0	20.23	1	868.7	-340.3
24	0.21	220	0.15	0.37	0.27	0.34	572.93	6717	5372		0	20.44	1	864.6	-291.7
25	0.22	220	0.16	0.37	0.27	0.35	534.23	6795	5345		0	21.23	1	893.1	-358.9
26	0.22	220	0.15	0.37	0.27	0.35	494.64	7088	5574		0	20.92	1	892.2	-397.5
27	0.22	220	0.16	0.37	0.27	0.35	462.61	7101	5285		0	21.02	1	882.4	-419.8
28	0.23	220	0.16	0.37	0.27	0.36	588.05	6830	5578		0	21.59	1.045	929.9	-341.9
29	0.36	160	0.29	0.38	0.26	0.51	1623.15	6993	5366		0	20.82	1.636	1305.3	327
30	0.36	160	0.30	0.38	0.26	0.51	1805.97	7203	5479		0	20.92	1.636	1316.7	489.3
31	0.14	110	0.12	0.38	0.26	0.31	252.66	6968	5218		0	8.68	1	455.0	-202.3
32	0.13	110	0.11	0.38	0.26	0.30	262.44	6907	5496		0	8.60	1	465.8	-203.3
33	0.17	110	0.15	0.38	0.26	0.34	380.77	6865	5140		0	9.69	1	481.9	-101.2
34	0.16	110	0.14	0.38	0.26	0.34	446.15	7068	5539		0	9.76	1	503.1	-56.9
35	0.18	110	0.15	0.38	0.26	0.35	287.80	6759	5281		0	9.96	1	497.3	-209.5

Row															
36	0.16	110	0.14	0.38	0.26	0.33	497.31	7199	5428	0	9.63	0	1	493.8	3.5
37	0.16	230	0.12	0.38	0.26	0.31	1398.07	6898	5362	0	18.73	0	1	800.5	597.6
38	0.13	230	0.10	0.38	0.26	0.27	258.44	7196	5609	0	16.60	0	1	735.1	-476.7
39	0.19	230	0.14	0.38	0.26	0.33	1266.85	7005	5130	0	20.23	0	1	845.0	421.8
40	0.11	230	0.08	0.38	0.26	0.25	567.59	7200	5839	0	15.19	0	1	696.5	-128.9
														Average:	145.6

CIV (1988 and 1989)

Row															
41	0.13	75	0.12	0.36	0.25	0.30	125	6174	0	0	5.63	0	1	120.1	4.9
42	0.13	75	0.11	0.35	0.27	0.29	76	6174	0	0	5.84	0	1	125.8	-49.8
43	0.10	70	0.09	0.36	0.25	0.26	58	6174	0	0	4.69	0	1	95.3	-37.3
44	0.10	70	0.09	0.35	0.27	0.26	125	6174	0	0	4.86	0	1	99.8	25.2
45	0.09	148	0.08	0.36	0.25	0.24	305	6174	0	0	8.97	0	1	215.9	89.1
46	0.09	148	0.08	0.35	0.27	0.23	247	6174	0	0	9.26	0	1	224.7	22.3
47	0.25	190	0.20	0.36	0.25	0.40	1021	6174	0	0	19.39	0	1.136	570.3	450.7
48	0.32	190	0.26	0.35	0.27	0.45	1085	6174	0	0	22.90	0	.455	483.2	201.8
49	0.22	190	0.18	0.36	0.25	0.37	721	6174	0	0	18.06	0	1	521.4	199.6
50	0.16	190	0.13	0.35	0.27	0.31	696	6174	0	0	15.64	0	1	434.9	261.1
51	0.18	200	0.14	0.36	0.25	0.33	716	6174	0	0	16.93	0	1	480.6	235.4
52	0.27	200	0.21	0.35	0.27	0.41	894	6174	0	0	21.78	0	1.227	660.0	234.0
53	0.21	265	0.15	0.36	0.25	0.34	1079	6174	0	0	23.14	0	1	712.6	366.4
54	0.21	265	0.15	0.35	0.27	0.33	801	6174	0	0	23.67	0	1	733.2	67.8
55	0.08	90	0.07	0.38	0.26	0.23	136	7171	0	0	5.35	0	1	112.7	23.3
56	0.06	95	0.06	0.33	0.16	0.19	102	7171	0	0	2.86	0	1	51.2	50.8
57	0.08	125	0.07	0.35	0.27	0.23	158	7171	0	0	7.73	0	1	179.1	-21.1
58	0.12	110	0.11	0.38	0.26	0.29	200	7171	0	0	8.25	0	1	194.3	5.7
59	0.12	110	0.11	0.33	0.16	0.28	89	7171	0	0	4.73	0	1	96.4	-7.4
60	0.12	110	0.10	0.35	0.27	0.28	245	7171	0	0	8.30	0	1	195.7	49.3
61	0.17	120	0.15	0.38	0.26	0.35	274	7171	0	0	10.90	0	1	275.9	-1.9
62	0.28	120	0.25	0.37	0.16	0.43	509	7171	0	0	8.14	0	1.273	278.0	91.6
63	0.22	120	0.20	0.35	0.27	0.39	432	7171	0	0	12.88	0	1	340.4	91.6
64	0.26	170	0.22	0.33	0.16	0.41	1026	7171	0	0	10.77	0	1.182	339.7	686.3
65	0.25	120	0.23	0.33	0.16	0.41	776	7171	0	0	7.70	0	1.136	222.6	553.3
66	0.21	170	0.17	0.35	0.27	0.36	905	7171	0	0	16.97	0	1	481.9	423.1
67	0.17	120	0.15	0.35	0.27	0.34	430	7171	0	0	11.09	0	1	282.0	148.0
68	0.20	170	0.16	0.38	0.26	0.36	747	7171	0	0	15.99	0	1	447.2	299.8
69	0.19	120	0.17	0.38	0.26	0.37	601	7171	0	0	11.43	0	1	293.0	308.0
70	0.20	120	0.17	0.38	0.26	0.38	767	7171	0	0	11.76	0	1	303.5	463.5
71	0.20	120	0.17	0.38	0.26	0.38	724	7171	0	0	11.76	0	1	303.5	420.5
72	0.20	120	0.17	0.38	0.26	0.38	918	7171	0	0	11.76	0	1	303.5	614.5
														Average:	175.4

HMMWV (1988 and 1989)

Row															
73	0.05	550	0	0.43	0.33	0	452	7228	9497	0	0	0	1	0.0	452.0
74	0.04	60	0.03	0.43	0.33	0.17	452	7228	9497	0	3.32	0	1	512.8	-60.8
75	0.12	75	0.11	0.43	0.33	0.31	786	7228	9497	0	7.73	0	1	630.1	155.9

76	0.09	148	0.07	0.43	0.33	0.25	1120	7228	9497	0	0	12.44	1	777.0	343.0
77	0.11	80	0.10	0.43	0.33	0.30	452	7228	9497	0	0	7.85	1	633.6	-181.6
78	0.31	220	0.23	0.43	0.33	0.46	1956	7228	9497	0	0	33.49	1.409	1771.0	185.0
79	0.22	250	0.15	0.43	0.33	0.37	1288	7228	9497	0	0	30.70	1	1468.4	-180.4
80	0.30	290	0.19	0.43	0.33	0.42	1790	7228	9497	0	0	40.42	1.364	2054.1	-264.1
81	0.18	148	0.15	0.43	0.33	0.37	786	7228	9497	0	0	17.87	1	965.6	-179.6
82	0.17	240	0.12	0.43	0.33	0.33	1622	7228	9497	0	0	25.95	1	1274.4	347.6
83	0.13	220	0.09	0.43	0.33	0.29	1388	7228	9497	0	0	20.80	1	1074.2	313.8
84	0.11	240	0.08	0.43	0.33	0.27	770	7228	9497	0	0	21.08	1	1084.5	-314.5
85	0.24	250	0.16	0.43	0.33	0.39	1956	7228	9497	0	0	31.80	1.091	1555.7	400.3
86	0.20	250	0.14	0.43	0.33	0.36	802	7228	9497	0	0	29.41	1	1414.9	-612.9
87	0.21	250	0.14	0.43	0.33	0.36	1054	7228	9497	0	0	29.64	1	1424.5	-370.5
88	0.06	360	0.03	0.43	0.33	0.13	200	7228	9497	0	0	23.33	1	1163.9	963.9
89	0.12	180	0.09	0.43	0.33	0.29	1120	7228	9497	0	0	17.11	1	938.1	181.9
90	0.06	360	0.02	0.43	0.33	0.13	384	7228	9497	0	0	23.35	1	0.0	384.0
91	0.04	120	0.03	0.43	0.33	0.17	618	7228	9497	0	0	6.81	1	603.7	14.3
92	0.15	160	0.12	0.43	0.33	0.33	836	7228	9497	0	0	17.37	1	0.0	836.0
93	0.18	160	0.14	0.43	0.33	0.36	1456	7228	9497	0	0	19.13	1	1011.7	444.3
94	0.15	190	0.11	0.43	0.33	0.32	904	7228	9497	0	0	20.12	1	1048.4	-144.4
														Average:	45.1

HEMTT (1988 and 1989)

95	0.04	60	0.03	0.62	0.43	0.20	2552	31004	31459	35786	36030	5.22	1	2483.7	68.3
96	0.04	60	0.03	0.59	0.48	0.20	2552	31004	31459	35786	36030	5.74	1	2497.6	54.4
97	0.10	75	0.09	0.62	0.43	0.34	1476	31004	31459	35786	36030	11.03	1	2654.9	-1178.9
98	0.10	75	0.09	0.59	0.48	0.34	2956	31004	31459	35786	36030	12.14	1	2690.6	265.4
99	0.11	80	0.10	0.62	0.43	0.36	3760	31004	31459	35786	36030	12.33	1	2696.9	1063.1
100	0.11	80	0.10	0.59	0.48	0.35	4296	31004	31459	35786	36030	13.56	1	2738.0	1558.0
101	0.25	220	0.20	0.62	0.43	0.51	3760	31004	31459	35786	36030	47.98	1.136	4483.4	-723.4
102	0.25	220	0.20	0.59	0.48	0.51	336	31004	31459	35786	36030	52.7	1.136	3707.4	4571.4
103	0.18	200	0.15	0.62	0.43	0.43	3760	31004	31459	35786	36030	37.16	1	3668.8	91.2
104	0.18	200	0.15	0.59	0.48	0.42	2016	31004	31459	35786	36030	40.81	1	3831.1	-1815.1
105	0.20	250	0.15	0.59	0.48	0.43	5104	31004	31459	35786	36030	52.19	1	4360.0	744.0
106	0.21	250	0.16	0.62	0.43	0.45	4028	31004	31459	35786	36030	48.79	1	4198.3	-170.3
107		360		0.62	0.43		2148	31004	31459	35786	36030		1	0.0	3148.0
108	0.05	230	0.04	0.62	0.43	0.22	2284	31004	31459	35786	36030	21.79	1	3035.1	-751.1
109	0.06	360		0.62	0.43		2148	31004	31459	35786	36030		1	0.0	3148.0
110	0.06	360		0.59	0.48		1344	31004	31459	35786	36030		1	0.0	1344.0
111	0.02	220	0.02	0.62	0.43	0.14	1476	31004	31459	35786	36030	13.22	1	2726.5	-1250.5
112	0.08	190	0.07	0.62	0.43	0.29	2416	31004	31459	35786	36030	23.40	1	3097.2	-681.2
113	0.13	210	0.10	0.62	0.43	0.36	3624	31004	31459	35786	36030	32.49	1	3467.2	156.8
														Average:	-171.2

LAV (1988)

114	0.05	550	0	0.45	0.35	0	732.90	16103	17281	34501	44557	0.0	1	0.0	752.9
115	0.05	550	0	0.42	0.34	0	815.65	16103	17281	34501	44557	0.0	1	0.0	815.7

116	0.04	60	0.03	0.45	0.35	0.17	1254.85	16103	17281	14501	14857	3.63	1	1246.7	8.1
117	0.04	60	0.03	0.42	0.38	0.17	815.65	16103	17281	14501	14857	3.75	1	1249.4	-433.8
118	0.12	75	0.11	0.45	0.35	0.32	1066.60	16103	17281	14501	14857	8.46	1	1378.2	-311.6
119	0.12	75	0.11	0.42	0.38	0.31	376.45	16103	17281	14501	14857	8.73	1	1386.1	-1009.6
120	0.11	80	0.10	0.45	0.35	0.31	1882.25	16103	17281	14501	14857	8.60	1	1382.2	500.0
121	0.11	80	0.10	0.42	0.38	0.29	2948.85	16103	17281	14501	14857	8.86	1	1390.2	1558.6
122	0.11	80	0.10	0.45	0.35	0.30	1882.25	16103	17281	14501	14857	8.60	1	1382.2	500.0
123	0.11	80	0.10	0.42	0.38	0.29	3074.35	16103	17281	14501	14857	8.86	1	1390.2	1684.1
124	0.11	150	0.09	0.45	0.35	0.29	1882.25	16103	17281	14501	14857	15.38	1	1603.6	278.7
125	0.11	150	0.09	0.42	0.38	0.28	3827.25	16103	17281	14501	14857	15.78	1	1617.4	2209.9
126	0.30	290	0.20	0.45	0.35	0.44	6274.20	16103	17281	14501	14857	45.31	1.364	3267.7	3006.5
127	0.30	290	0.19	0.42	0.38	0.42	2760.65	16103	17281	14501	14857	45.88	1.364	3294.1	-533.4
128	0.23	250	0.17	0.45	0.35	0.40	4956.60	16103	17281	14501	14857	35.03	1.045	2431.9	2524.7
129	0.23	250	0.16	0.42	0.38	0.38	4454.65	16103	17281	14501	14857	35.63	1.045	2457.8	1996.9
130	0.30	290	0.23	0.43	0.31	0.48	2392.70	15346	16481	13823	14168	42.23	1.364	3051.9	-659.2
131	0.30	290	0.22	0.42	0.33	0.45	2990.85	15346	16481	13823	14168	43.02	1.364	3088.1	-97.2
132	0.23	250	0.18	0.43	0.33	0.41	8314.60	15346	16481	13823	14168	32.25	1.045	2336.2	6083.2
133	0.23	250	0.18	0.42	0.33	0.40	2751.60	15346	16481	13823	14168	32.98	1.045	2286.7	464.9
134	0.30	270	0.23	0.43	0.31	0.47	2273.05	15346	16481	13823	14168	39.81	1.364	2943.2	-670.1
135	0.30	270	0.22	0.42	0.33	0.45	2631.95	15346	16481	13823	14168	40.64	1.364	2980.0	-348.1
136	0.03	550	0	0.44	0.31	0	1973.95	15346	16481	13823	14168	0.0	1	0.0	1974.0
137	0.03	550	0	0.44	0.33	0	3330.15	15346	16481	13823	14168	0.0	1	0.0	3330.2
138	0.30	290	0.22	0.42	0.33	0.45	2871.20	15346	16481	13823	14168	43.65	1.364	3116.5	-245.3
														Average:	496.5

5-Ton Truck (1988)

139	0.30	80	0.27	0.55	0.41	0.57	476	23842	14523	14523	0	18.73	1.364	1974.0	-1498.0
140	0.25	220	0.18	0.55	0.41	0.47	2432.90	23842	14523	14523	0	41.81	1.136	2929.5	-496.6
141	0.18	200	0.14	0.55	0.41	0.40	846.25	23842	14523	14523	0	32.50	1	2140.4	-1294.1
														Average:	-1096.2

Note: the shaded data was not included in the regression analysis nor in the average residuals for the following reasons:

1. If the sinkage is greater than 2/3 the radius, then this is considered deep snow (Richmond et al., (in prep.)) for the these cases the predicted shallow snow resistance is multiplied by 1.25.

2. If the initial density is ≥ 550 than this is packed snow and the resistance is assumed to be zero, measured values could be do to surface roughness.

3. Two data sets, nos. 102 and 132 were not included because they are clearly outliers, some error or undetected equipment failure may have occurred during testing.

REPORT DOCUMENTATION PAGE

1. AGENCY USE ONLY (Leave blank)	2. REPORT DATE March 1995	3. REPORT TYPE AND DATES COVERED

4. TITLE AND SUBTITLE
Motion Resistance of Wheeled Vehicles in Snow

5. FUNDING NUMBERS
PR: 4A762784AT42
TA: CS
WU: M04

6. AUTHORS
Paul W. Richmond

7. PERFORMING ORGANIZATION NAME(S) AND ADDRESS(ES)
U.S. Army Cold Regions Research and Engineering Laboratory
72 Lyme Road
Hanover, N.H. 03755-1290

8. PERFORMING ORGANIZATION REPORT NUMBER
CRREL Report 95-7

9. SPONSORING/MONITORING AGENCY NAME(S) AND ADDRESS(ES)
Office of the Chief of Engineers
Washington, DC 02314-1000

10. SPONSORING/MONITORING AGENCY REPORT NUMBER

11. SUPPLEMENTARY NOTES

12a. DISTRIBUTION/AVAILABILITY STATEMENT
Approved for public release; distribution is unlimited.
Available from NTIS, Springfield, Virginia 22161

12b. DISTRIBUTION CODE

13. ABSTRACT (Maximum 200 words)

Before vehicle mobility in snow can be reliably predicted, a complete understanding of motion resistance in snow is required. This report examines several aspects of wheeled vehicle motion resistance using results obtained with the CRREL instrumented vehicle. Resistances of leading and trailing tires are examined. Limited data are presented for undercarriage drag, and third and fourth wheel passes in the same rut are initially analyzed, as is how snow deforms around a wheel. For the CRREL instrumented vehicle, a trailing tire has a resistance coefficient of about 0.017 for snow depths less than about 22 cm. For deeper snow, the disruption of the snowpack caused by a preceding wheel causes snow to fall into the rut, resulting in higher trailing tire coefficients. For larger vehicles, which in some cases have trailing tires carrying larger loads than preceding tires, the trailing tire coefficients are on the order of 0.048 and 0.025 for second and third trailing wheels respectively. Since there are no trailing tire data available for these larger vehicles, these values are based on nonlinear regression analysis, which includes a prediction of the leading tire resistance. The results and observations of this study are applied in a reanalysis of the towed resistance data obtained during the U.S. Army's Wheels vs. Tracks study. An improved algorithm is presented for predicting wheeled vehicle motion resistance caused by snow.

14. SUBJECT TERMS

Instrumented vehicles	Snow	Vehicles
Mobility predictions	Snow strength	Trafficability
Motion resistance	Vehicle traction	Off road mobility

15. NUMBER OF PAGES 47

16. PRICE CODE

17. SECURITY CLASSIFICATION OF REPORT	18. SECURITY CLASSIFICATION OF THIS PAGE	19. SECURITY CLASSIFICATION OF ABSTRACT	20. LIMITATION OF ABSTRACT
UNCLASSIFIED	UNCLASSIFIED	UNCLASSIFIED	UL